1 **Biogeochemical relationships between ultrafiltered dissolved organic matter and**

2 **picoplankton activity in the Eastern Mediterranean Sea**

3

4 *Travis B. Meador[a,b,g]*, Alexandra Gogou[a,b], Georgina Spyres[a,c], Gerhard J. Herndl[d,e], Evangelia*

5 *Krasakopoulou[a], Stella Psarra[f], Taichi Yokokawa[c], Daniele De Corte[c,e], Vassilis Zervakis[b],*

6 *Daniel J. Repeta[g]*

7 [a]Hellenic Centre for Marine Research, Institute of Oceanography, 46.7 km Athens-Sounion Av.,

8 19013 Anavyssos, Greece.

9 [b]University of the Aegean, Department of Marine Sciences, 81100 Mytilene, Lesvos, Greece.

10 [c]Dept. of Biological Oceanography, Royal Netherlands Institute for Sea Research (NIOZ), PO

11 Box 59, 1790AB Den Burg, The Netherlands.

12 [d]Univ. of Vienna, Ecology Center, Dept. of Marine Biology, Althanstr. 14, 1090 Vienna, Austria

13 [e]Center for Ecological and Evolutionary Studies, University of Groningen, PO Box 14, 9750 AA

14 Haren, The Netherlands

15 [f]Hellenic Center for Marine Research, Institute of Oceanography, 71003 Heraklion, Crete,

16 Greece

17 [g]Department of Marine Chemistry and Geochemistry, Woods Hole Oceanographic Institution,

18 Woods Hole, Massachusetts 02543, USA

19

20 running head: DOM reactivity in the Eastern Mediterranean Sea

21

22

23 *Corresponding author.

24 [1]Present address: Department of Marine Chemistry and Geochemistry, Woods Hole

25 Oceanographic Institution, Woods Hole, Massachusetts 02543, USA

26 Tel.: 508-289-3955 fax: 508-457-2075

27 E-mail address: tmeador@whoi.edu (T.B. Meador)

28

29

30

31

32

33

34

Abstract

We targeted the warm, subsurface waters of the Eastern Mediterranean Sea (EMS) to investigate processes that are linked to the chemical composition and cycling of dissolved organic carbon (DOC) in seawater. The apparent respiration of semi-labile DOC accounted for 27 ± 18% of oxygen consumption in EMS mesopelagic and bathypelagic waters; this value is higher than that observed in the bathypelagic open ocean, so the chemical signals that accompany remineralization of DOC may thus be more pronounced in this region. Ultrafiltered dissolved organic matter (UDOM) collected from four deep basins at depths ranging from 2 to 4350 m exhibited bulk chemical (^{1}H-NMR) and molecular level (amino acid and monosaccharide) abundances, composition, and spatial distribution that were similar to previous reports, except for a sample collected in the deep waters of the N. Aegean Sea that had been isolated for over a decade. The amino acid component of UDOM was tightly correlated with apparent oxygen utilization and prokaryotic activity, indicating its relationship with remineralization processes that occur over a large range of timescales. Principal component analyses of relative mole percentages of monomers revealed that oxygen consumption and prokaryotic activity were correlated with variability in amino acid distributions but not well correlated with monosaccharide distributions. Taken together, this study elucidates key relationships between the chemical composition of DOM and heterotrophic metabolism.

Key words: DOM, biogeochemical cycles, ultrafiltration, AOU, microbial loop

1. Introduction

1.1. Dissolved organic matter (DOM) cycling

Oceanic dissolved organic carbon (DOC) is one of the largest reservoirs of carbon on Earth, and its potential for exchange with other carbon reservoirs has brought it within the focus of global carbon cycle research (Williams and Druffel, 1988; Toggweiler, 1989; Hedges, 1992; Hansell, 2002). The euphotic zone is the principal site of organic matter production in the open ocean. The magnitude and composition of DOM produced during bloom events vary considerably and are controlled by a number of biological, chemical and physical parameters (Carlson, 2002). In the surface ocean, DOC stocks exceeding the deep refractory pool are composed of 'labile' and 'semi-labile' DOC (Hansell and Carlson, 1998a). Because labile DOC concentrations represent a very small fraction of bulk DOC (0-6%), the vertical gradient of the bulk DOC observed in stratified systems is mostly comprised of 'semi-labile' DOM (Carlson and Ducklow, 1995;

1 Cherrier et al., 1996). The labile component of DOC arising from autotrophic production in the

2 surface ocean is thought to support production of heterotrophic bacterioplankton (i.e., the

3 microbial loop; Azam et al., 1983), and is either repackaged into bacterial organisms and passed

4 to higher trophic levels or remineralized. Semi-labile DOC escapes rapid degradation by marine

5 heterotrophs in surface ocean waters and so is available for export to the ocean's interior by

6 convective mixing (Copin-Montegut and Avril, 1993; Carlson et al., 1994), advection along

7 isopycnals surfaces (Hansell and Carlson, 2001), or sorption onto sinking particles (Keil and

8 Kirchman, 1994; Druffel et al., 1996. This fraction can amount to 1.2 Gt C yr^{-1}, or 17% of global

9 new production (Hansell and Carlson, 1998b) and provides a carbon source that fuels production

10 by deep-sea free-living prokaryotes (Karner and Herndl, 1992; Smith et al., 1992; Nagata et al.,

11 2000; Nagata et al., 2010).

12

13 *1.2 Oceanographic setting*

14

15   The Mediterranean Sea has often been described as a small ocean as it encompasses all

16 oceanic processes at much smaller time and space scales (Béthoux et al., 2002). Its thermohaline

17 cell is forced by deep water formation at the northern coasts of the Mediterranean during winter,

18 and the formation of Levantine Intermediate waters in the northern part of the Eastern

19 Mediterranean. In its eastern part, the Eastern Mediterranean Sea (EMS) is an ultra-oligotrophic

20 environment characterized by extremely low dissolved nutrient concentrations, chlorophyll-a

21 concentrations, and phytoplankton biomass in surface waters (Krom et al., 2003). The EMS is

22 unique among the oligotrophic oceans because the ratio between dissolved nitrate and phosphate

23 is higher than 20 in all sub-thermocline water masses (Krom et al.,1992; Béthoux et al., 2002). Its

24 annual primary productivity is 60-80 g C m^{-2} y^{-1} (Ignatiades, 1998; Psarra et al., 2000),

25 approximately half that determined in the oligotrophic Sargasso Sea (e.g., 157 ± 7 g C m^{-2} y^{-1},

26 Brix et al., 2006).

27   The area under investigation in this study extends throughout the Aegean Sea and into the

28 Cretan and Ionian Seas (Fig. 1). Complex sea-bed topography together with Black Sea Waters

29 (BSW) entering through the Dardanelles Straits and highly saline waters of Levantine origin

30 determine the structure of the water column in the Aegean and, partly, the Ionian Seas. The

31 surface layer of the north – northwest Aegean is covered by a light, thin layer of Black Sea Water

32 of salinity as low as 30-35. The depths between 70 and 400 m in the North Aegean are waters

33 with southeast Aegean / Levantine origin and are identified as the Levantine Intermediate Water

1   (LIW; Lascaratos, 1993; Tzipperman and Speer, 1994), the most voluminous water mass of the

2   Mediterranean (estimated at 2-3.5 x 10^{13} m^3; Myers and Haines, 2000).

3   Below the LIW, the deep basins of the North Aegean are filled with locally-formed North

4   Aegean Deep Water (NAeDW). These waters form at infrequent intervals, as their high density

5   hinders renewal and ventilation. The current NAeDW was formed during two major dense water

6   formation events in the winters of 1992 and 1993 (Zervakis et al., 2000). Since then, the

7   properties have evolved as a result of turbulent vertical mixing with the overlying LIW (Zervakis

8   et al., 2003). During mild winters, LIW in the northeastern Aegean can be further subducted in an

9   annual process that contributes to the formation Cretan Deep Water (CDW) (Zervakis et al.,

10   2004; Gertman et al., 2006). The latter water mass thus contains higher dissolved oxygen than the

11   deep layer of the North Aegean. Comparative analysis of T/S diagrams (see also Fig. 2b) suggests

12   a significant contribution of North Aegean Sea water to CDW.

13   The layers between 400 and 900 m in the South Aegean (Cretan Sea) are characterized by

14   a salinity minimum, signifying the Transitional Mediterranean Water mass (TMW), a mixture of

15   LIW and Eastern Mediterranean Deep Waters (EMDW), the bottom waters of the Eastern

16   Mediterranean found in the Ionian and Levantine Seas. TMW enters the Cretan Sea through the

17   Cretan Straits, and its signature in the Cretan Sea is stronger when the exchange through the

18   Straits intensifies. In this region above 400 m, a salinity maximum identifies the Cretan

19   Intermediate Water, a locally formed water analogous to LIW, but with higher salinity. Lower

20   salinities often found at the surface have been attributed to the inflow of Atlantic water through

21   the Cretan Straits (Theocharis et al., 1999) and more recently to BSW (Zervakis et al., 2002).

22   The water column in the Ionian Sea is composed of a surface water mixture of Levantine,

23   Cretan Sea, and Atlantic Waters, a LIW layer down to about 700 m, the TMW mass between 800

24   and 1000 m, and the EMDW masses, which comprise deep water of different origins formed

25   during different generations of the Eastern Mediterranean Transient (Roether et al., 2007). The

26   TMW mass, both in and outside the Cretan Sea, is probably the oldest of all types of water found

27   in the region as it consists of a mixture of LIW with the oldest EMDW.

28

29   *1.3 Objective*

30

31   Previous reports have noted the inventory of total organic carbon (TOC) in the

32   Mediterranean Sea (about 3 Pg C; Sempéré et al., 2000) and an average turnover time of "excess

33   TOC" (i.e., semi-labile TOC) of 0.47 years in the N. Aegean and 0.28 years in the S. Aegean Seas

34   (Sempéré et al., 2002). Additional details of the processes that control DOM reactivity in the

EMS could be revealed by simultaneous measurements of DOM and microbial composition. In this study, we determined the total bulk chemical composition (inorganic nutrients, DOC), prokaryotic abundance and molecular-level chemical composition of UDOM in order to investigate the biological and chemical signatures that accompany respiration and the turnover of marine UDOM in this unique, oligotrophic marine environment. Emphasis is put on DOM production and degradation processes that occur in the mesopelagic (200 to 1000 m) and bathypelagic waters (> 1000 m) of the EMS, which exhibit higher temperatures (> 13°C), higher oxygen consumption rates (0.53 μmol O_2 kg^{-1} y^{-1}; Roether and Well, 2001) and enhanced microbial activity relative to the bathypelagic Atlantic (Martín-Cuadrado et al., 2007). Our sample set includes depths to 4350 m, but we categorize samples as representative of either surface or subsurface waters (i.e., above or below the euphotic zone, respectively), paralleling the surface and mesopelagic realms of the open ocean.

We collected ultrafiltered DOM (UDOM; > 500 Da) from eight distinct water masses in the EMS. This approach is one of only a few methods that isolates DOM from the more abundant salts in seawater, thus permitting enhanced chemical characterization of the high molecular weight (HMW) component of DOM (e.g., Benner et al., 1992; McCarthy et al., 1996; Aluwihare et al., 1997; Aluwihare et al., 2002; Meador et al., 2007). Correlations between apparent oxygen utilization (AOU) and TOC were used to estimate the proportion of carbon demand supported by TOC, and the molecular level composition of UDOM was determined to identify the chemical alterations that accompany the removal of the 'semi-labile' pool of DOC (also 'exportable TOC', Hansell, 2002; and 'excess TOC', Sempéré et al., 2002) that escapes degradation in surface waters. Also, direct comparisons are drawn between the bulk chemical (e.g., ^{1}H-NMR) and molecular level composition (e.g., amino acid and monosaccharide distribution) of UDOM and local prokaryotic abundance and productivity. This analysis serves to further delineate the linkages between microbial metabolism and UDOM degradation processes in the ultra-oligotrophic and net heterotrophic Eastern Mediterranean basin.

2. Methods

2.1 Sampling

Samples were collected onboard the oceanographic vessel R/V AEGAEO, during the POSEIDON (May 2007), SESAME (April 2008) and KM3Net (April 2008) cruises. A SBE-9

1 Plus Sea-Bird CTD profiler was used for data acquisition; this was equipped with pressure,

2 temperature, conductivity, dissolved oxygen, fluorescence and light transmission sensors. The

3 CTD salinity data were calibrated against water sample salinity measured using an AUTOSAL

4 salinometer. The CTD profiler was mounted on a 24-Niskin-bottle rosette sampler, used to obtain

5 sub-surface water samples. Surface water samples were collected using an air-pressure driven

6 membrane pump and Teflon® tubing. Eight stations (Fig. 1) were selected in sub-basins in the

7 north and south Aegean Sea and the southeastern Ionian Sea to represent various water masses of

8 the E. Mediterranean. UDOM samples were collected at depths ranging from 2 to 4350 m at four

9 stations during the POSEIDON cruise in May 2007 (station names: N. Aegean, S. Aegean, SW

10 Aegean and Ionian; Table 1). At these stations, samples were also collected to determine depth

11 profiles of inorganic nutrients (i.e., DIN, DIP), organic matter (i.e., TOC, UDOM chemical

12 characterization) and biological parameters including prokaryotic abundance and activity, and

13 community structure.

14

15 *2.2 Inorganic Nutrients*

16

17   Nutrient samples were collected in pre-cleaned polyethylene bottles and stored at -20ºC

18 until analysis in the laboratory. Dissolved inorganic nitrogen (DIN) was measured with a

19 Bran+Luebbe II autoanalyzer following the method described by Strickland and Parsons (1972).

20 Phosphate (DIP) was measured with a Perkin Elmer 20 Lambda UV/VIS Spectrometer according

21 to the method of Murphy and Riley (1962).

22

23 *2.3 Dissolved Organic Carbon (DOC)*

24

25 For DOC determination, unfiltered samples from >150m were pipetted into combusted (450°C

26 for 4 h) glass ampoules, immediately acidified with 3 to 4 drops of 45 % H_3PO_4 and then flame

27 sealed. Surface water samples collected above 150m were filtered through rinsed 0.2 µm

28 polycarbonate filters. Samples were stored at −20°C until analysis. DOC analysis was performed

29 using the high temperature combustion method on a modified Shimadzu TOC-5000A (Hansell,

30 1993; Spyres et al., 2000). The sample was automatically injected in quadruplicate onto a

31 platinized aluminum catalyst at a combustion temperature of 680°C. DOC concentrations in

32 samples were determined relative to standards prepared using potassium hydrogen phthalate in

33 Milli-Q water and consensus reference materials for DOC provided by the NSF-CRM program

34 (http://www.rsmas.miami.edu/groups/biogeochem/CRM.html). The overall analytical precision

1   was always < 3 %. For simplicity, we use the term DOC when referring specifically to the

2   measurements of both the filtered (surface) and un-filtered samples (see Hansell 2002), and in

3   reference to the more abstract global reservoir of carbon.

4

5   *2.4 Dissolved Oxygen*

6

7   Samples for the determination of oxygen were first taken from the Niskin bottles with the

8   recommended precautions to prevent any biological activity and gas exchange with the

9   atmosphere, and titrated immediately afterward using a Dosimat Metrohm according to the

10   Winkler method (Carpenter, 1965a, b). This method was consistent with other determinations of

11   oxygen in seawater; the precision of the method was ~2.2 µmol O_2 L^{-1} (Klein et al., 2003). The

12   apparent oxygen utilization (AOU) was calculated according to the difference of the measured

13   oxygen values to the oxygen saturation given by the Benson and Krause equation (UNESCO

14   1986).

15

16   *2.5 Enumeration of picoplankton*

17

18   Picoplankton abundance was determined in seawater collected from the Niskin bottles and

19   fixed with 0.2 µm filtered formaldehyde (2% final concentration). Thereafter, the samples were

20   frozen in liquid nitrogen for 10 min, then kept at –80°C until analysis. Picoplankton abundance

21   was determined by flow cytometry within two months of collection. Samples were thawed to

22   room temperature and 0.5 mL subsamples were stained with SYBR Green I in the dark for 10

23   min; subsequently, 1 µm fluorescent latex beads (Molecular Probes) (approximately 10^5 mL^{-1})

24   were added to the samples as internal standard. The picoplankton were enumerated on a

25   FACScalibur flow cytometer (Becton Dickinson) by their signature in a plot of green

26   fluorescence versus side scatter, and the abundance was calculated based on the ratio of stained

27   cells to the internal standard. To convert cell abundance to picoplankton carbon biomass, a

28   carbon content of 20 fg C $cell^{-1}$ was used (Fukuda et al., 1998); this conversion likely

29   overestimates picoplankton biomass but is used as a conservative estimate in terms of considering

30   the possibility of contamination of DOC measurements by C directly associated with

31   picoplankton biomass.

32

33   *2.6 Prokaryotic activity*

34

1   ^{3}H-leucine incorporation rates were determined as a proxy for heterotrophic prokaryotic

2   production (Kirchman, 2001). Subsamples (5 – 40 mL) from each depth were amended with 5

3   nmol L^{-1} ^{3}H-leucine (Amersham, specific activity: 160 Ci $mmol^{-1}$) and incubated at in situ

4   temperature ($\pm$ 1°C) in the dark. Incubation time varied depending on depth: 1h for upper waters

5   (<100 m) and 24h for deep waters (>100 m). After incubation, samples were filtered onto

6   polycarbonate filters (pore size, 0.2 μm, Millipore) and rinsed twice with both 5% trichloroacetic

7   acid and 80% ethanol. The samples were radio-assayed with a liquid scintillation counter (1211

8   Rackbeta, Wallac) using FilterCount scintillation cocktail (Packard). Duplicate samples and one

9   trichloroacetic acid-killed control were prepared for each depth. The disintegrations per minute

10   (DPM) of the killed control were subtracted from the mean DPM of the corresponding duplicate

11   samples and the resulting count converted into leucine uptake rates.

12

13   *2.6 Ultrafiltration*

14

15   Water samples (150 to 300 L) collected during the POSEIDON May 2007 cruise were

16   prefiltered through 0.2 μm cartridge filters (Gelman Criticap, USA). Ultrafiltered dissolved

17   organic matter (UDOM) was obtained by concentrating these prefiltered samples using a custom-

18   made Amicon SP-60 tangential-flow ultrafiltration system equipped with a Kock (Germany)

19   spiral-wound polyamide 500 Dalton cut-off filter cartridge (operating pressure 3.0-5.5 bar, filter

20   area 7.9 m^2, filtrate flow rate 192 L h^{-1} at 3.0 bar) cleaned with 0.1 mol L^{-1} sodium hydroxide

21   between samples. The samples were concentrated to about 6 L and stored frozen at -20°C for

22   transport to the laboratory. Aliquots of ultrafiltered samples for amino acid analysis were

23   collected in precombusted glass vials, then flame sealed and frozen until analysis. In the

24   laboratory, most salts were removed from the concentrated samples by diafiltration with 10

25   volumes (i.e., 60 L) of MilliQ water, then lyophilized to a dry powder. UDOM samples that were

26   concentrated and frozen after collection during the spring 2007 POSEIDON cruise exhibited a

27   high-salt precipitate when thawed for desalting. This precipitate was removed by filtering through

28   GF/F (Whatman) before diafiltration of the dissolved sample; we are unsure of the carbon content

29   of this precipitate.

30   Large volume seawater samples (150 to 200L) collected during the SESAME (NS1 and

31   NS6) and KM3Net (4.5 and C2) cruises were pumped exclusively from surface waters and

32   prefiltered through 0.5 μm (Millipore Opticap XL4, USA) and 0.2 μm cartridge filters (Domnick

33   Hunter, UK), then ultrafiltered using a 500 Da (nomimal molecular weight cutoff, MWCO) spiral

34   wound cartridge (Separation Engineering Inc. GE2540F1072, operating pressure <3.0 bar, filter

1 area 1.9 m^2, filtrate flow rate 30 L h^{-1}). Immediately after ultrafiltration, concentrated samples

2 were diafiltered with ~ 80L of MilliQ water; volumes were reduced to < 4L and stored at -20°C.

3 Frozen samples were lyophilized in the laboratory, or aliquots of concentrated UDOM solution

4 were used for composition analyses.

5

6 *2.6.1 Proton (^1H) Nuclear Magnetic Resonance (NMR) Spectroscopy*

7

8   Approximately 20 to 200 mg of dried UDOM samples were dissolved in 0.75mL of

9 deuterated water (D$_2$O) and ^{1}H-NMR spectra were determined on a 400MHz Bruker NMR with

10 typically > 2000 scans. The HDO peak was referenced to 4.76 ppm and was repressed in some

11 cases. ^{1}H-NMR spectra were integrated with Mestre-C software according to chemical shift

12 ranges defined as: aliphatic (C-C**H**-C, 0.5 to 1.8ppm), alpha-substituted (O-C-C**H**-C, 1.8 to

13 3.2ppm), and heteroatom substituted (O-C**H**-C or N-C**H**-C, 3.2 to 4.6ppm). Resonances that

14 appeared more downfield than 4.6ppm (e.g., protons attached to unsaturated or aromatic carbons),

15 were evident in some spectra, but were minimal and obscured by the peak arising from water;

16 these were excluded from the analysis.

17

18 *2.6.2 Monosaccharide analysis*

19

20   The distributions of individual monosaccharides were determined for UDOM samples

21 after diafiltration. Aliquots of UDOM samples representing 2.6 to 6.7 μmol C were hydrolyzed in

22 0.5mL 2 mol L^{-1} trifluoroacetic acid (TFA) with 40 μg mL^{-1} myo-inositol at 120°C for 2h.

23 Samples were then dried under a stream of N$_2$ gas and traces of acid were removed from the

24 hydrolysate with subsequent resuspension and evaporation of isopropanol. Monosaccharides were

25 reduced and acetylated to produce alditol acetates according to Aluwihare et al. (2002). Alditol

26 acetates were separated by gas chromatography with a 30 m HP-5 fused silica column, with on-

27 column injection at 270°C. After injection of 2 to 5μL of sample, the oven temperature was held

28 at 100°C for 1 min, then increased to 280°C at 3°C min^{-1}, and held at this temperature for the

29 final 8 min. Alternatively, samples were injected with an injection port temperature that followed

30 the oven gradient, holding at 50°C for 2 min, then ramping to 230°C at 5°C min^{-1}, then holding at

31 280°C for the final 8 min. Alditol acetates were identified by retention time and relative

32 abundances were determined by the FID response of standards. Monosaccharides identified in

33 this study included rhamnose (rham), fucose (fuc), arabinose (arab), xylose (xyl), mannose (man),

34 galactose (gal), and glucose (glc). We were unable to quantify total yields of alditol acetates as

1   the peak areas generated by monosaccharide standards were not reproducible; we attribute this

2   complication to the on-column injection and to the HP-5 column. We recommend using a

3   Supelco (SP2330) column with split injection. However, the relative peak areas of individual

4   monosaccharides in standard and sample replicate injections were consistent (± 0.6%), so we

5   report monosaccharide mole percentages of UDOM samples.

6   Carbohydrate abundances were determined using the TPTZ method of Myklestad et al.

7   (1997), modified by Panagiotopoulos and Sempéré (2005), after hydrolysis of UDOM in 2 mol L^{-1}

8   TFA at 120°C for 2 h. Aliquots of UDOM solutions used for this analysis ranged from 62 to 408

9   nmol C. Data are reported as dissolved combined neutral sugar concentration (DCNS) and as the

10   percent of UDOC that is neutral sugar carbon (%NS-UDOC)

11

12   *2.6.3 Amino acid analysis*

13

14   Samples were collected directly from the ultrafiltration system, pipetted into combusted

15   (450°C for 4 h) 10mL glass ampoules, flame sealed and stored frozen at –20°C for transport to

16   the laboratory for analysis. Samples were thawed and processed following the methodology of

17   Fitznar et al. (1999) and Pérez et al. (2003). Hydrolysis was performed by adding HCl and

18   ascorbic acid to 2mL of sample and subsequently flushing with N_2. The pre-combusted glass

19   ampoules were then sealed and incubated at 110°C for 24 h. The hydrolyzed samples were dried

20   and resuspended in a borate buffer (pH 8.5).

21   After hydrolysis, the concentrations of the individual amino acids were determined by

22   high performance liquid chromatography (HPLC) of duplicate injections after pre-column

23   derivatization with *o*-phthaldialdehyde and *N*-isobutyryl-L-cysteine (Fitznar et al., 1999; Pérez et

24   al., 2003). An integrated HPLC system was used consisting of a fluorescence detector (set at Ex:

25   330 nm; Em 445 nm) and autosampler for automatic derivatization. For separation of the

26   individual amino acids, we used a C-12 reversed phased column and solvents and a multistep

27   gradient system as described in Fitznar et al. (1999) as modified by Pérez et al. (2003). Amino

28   acids were identified and quantified in relation to external standards. The *N*-isobutyryl-D-

29   cysteine isomer was not used for derivitization as repeatable and clean chromatograms were

30   generated using this method. Using these conditions, we measured glycine (gly), the D and L-

31   enantiomers of aspartic acid and asparagine (asx, D-asx), glutamic acid and glutamine (glx, D-

32   glx), serine (ser, D-ser), alanine (ala, D-ala), and tyrosine (tyr, D-tyr), as well as the L-

33   enantiomers of threonine (thr), histidine (his), arginine (arg), valine (val), phenylalanine (phe),

34   and leucine (leu). Derivitized Thr and His residues co-eluted and are reported as a single peak.

Under these conditions, asparagine and glutamine were converted to aspartic and glutamic acid during acid hydrolysis and have the highest racemization rates. However, the development of this method involved a careful choice of reagents and solvents as well as adjustment of the pH in order to minimize the rate of racemization.

Data were corrected for both the blank and for racemization after hydrolysis (according to Kaiser and Benner 2005), and are reported as the total concentration of dissolved combined amino acids in seawater (DCAA), the percent of UDOC that is amino acid carbon (%AA-UDOC), and as mole percentages (mol%) of individual amino acids. The coefficient of variation for DCAA between duplicate samples ranged from 0.7 to 4.6%; the relative standard deviation for the individual amino acids in each run was < 6 %. It is possible that some amino acid peaks contained impurities, having significant implications for peaks with small areas. D-tyr peak areas were the smallest detected, but values were > 2× blank (except for the deep N. Aegean sample, which we have omitted) and we interpret these data with caution.

2.7 Principal Components Analysis

Principal components of amino acid and monosaccharide mol % data were determined using the Matlab statistics toolbox. Data were de-trended by removing the average and normalizing to the standard deviation for each variable prior to generating PCA data. Results are reported as PC loadings for individual amino acid or monosaccharide mol % variables, PC scores of UDOM samples, and z-scores of principal components identified in the datasets.

3. Results and Discussion

The exchange of carbon between CO_2 and the ocean's large reservoir of DOC has substantial implications for global biogeochemical cycles and global climate. We still know little regarding the routes and fluxes of DOC production and remineralization, particularly in the meso- and bathypelagic ocean. DOC removal processes in the EMS may differ from those in the open ocean as bathypelagic temperatures are > 13°C. Specifically, microbial remineralization processes that affect DOC concentration and/or composition in the meso- and bathypelagic Mediterranean waters may thus be more pronounced, and the chemical signatures of these processes may be more evident than in the major oceanic basins. For example, previous studies have noted the overwhelming presence of genes specific for the catabolism of amino acids and

11

1   carbohydrates down to 4000 m (Martín-Cuadrado et al., 2007), and correlations between DOC

2   and AOU have been shown to vary between water masses of the EMS (Seritti et al., 2003;

3   Santinelli et al. 2010).

4

5   *3.1 Water Mass Characteristics and Distributions of Bulk Chemical and Biological Parameters*

6

7   Sample locations and hydrographic parameters are reported in Table 1. We identified the

8   water masses sampled for UDOM according to their characteristic temperature and salinity

9   signatures (Fig. 2), along with additional variables such as dissolved oxygen and inorganic

10   nutrient concentrations (Tables 1 and 2). Specifically, we isolated UDOM from surface waters

11   containing MAW or BSW, subsurface intermediate waters of the LIW, CIW, and TMW (200 to

12   750 m), and NAeDW, CDW, and EMDW from the deep E. Mediterranean Sea (1200 to 4350 m).

13   Figure 2b provides an enhanced view of the relations between the intermediate and deep water

14   masses and types of the Aegean Sea. Note that the layer between 200 and 400 m in the North

15   Aegean has similar characteristics to 1000-1400 m deep waters in the Cretan Sea. Also, the TMW

16   and CIW waters seem to affect the shape of the T/S signature in the North Aegean.

17   AOU provides an estimate of the amount of oxygen consumed since a water parcel was at

18   the surface and hypothetically in gaseous equilibrium with the atmosphere (i.e., fully saturated in

19   oxygen). We observed significant variability in the AOU signature of water masses sampled in

20   this study (Table 1), which may correspond to variability in the extent of removal of semi-labile

21   DOC (Klein et al., 2003; Seritti et al., 2003; Santinelli et al., 2006). POC flux and the processes

22   associated with that flux attenuation could also affect AOU, but the EMS is one of the well-

23   known basins of low productivity of the world ocean; as such, organic particles are scarce in its

24   sub-surface layers (Stavrakakis et al., 2006; Karageorgis et al., 2008). Thus, the oxidation of POC

25   at depth could have had a minor effect on the levels of AOU and DOC, compared to that which

26   occurs in more productive ocean basins. Water mass mixing definitely altered the concentration

27   of both parameters and may have contributed to the observed variation in AOU and DOC

28   concentrations. Sampling for both dissolved oxygen and DOC was performed simultaneously in

29   the core of specific water masses that are characterized by different ages, sources, paths and

30   hydrochemical properties. Thus each data pair may provide a signature of the specific history and

31   path of the associated water mass.

32   Surface waters (0-100m) in all sampling locations were close to oxygen saturation or

33   even over-saturated, with AOU concentrations ranging between -8.9 and 33.3 µmol L^{-1}. Elevated

34   AOU values were observed at depths > 200 m, reflecting the history of the different water masses

1 occupying these layers. The highest AOU values (61.7-68.2 µmol L^{-1}) were recorded in the Ionian

2 Sea, at depths 750-1000 m, and represent TMW, an 'aged' water mass (see above). The lower

3 AOU (49.4 µmol L^{-1}) of the Levantine Intermediate waters, lying above the TMW layer, reveals

4 its recent ventilation with respect to TMW. Below TMW, at the depth range from 2000 to 4350

5 m, the AOU values decrease gradually, implying that the deepest EMDW is probably younger

6 (AOU of 49.0 µmol L^{-1}) than the EMDW of the overlying layers (AOU of 58.2 - 53.4 µmol L^{-1}).

7 In the N. Aegean, the NAeDW, which has remained isolated since the major deep water

8 formation event of winter 1993 (Zervakis et al., 2003), is characterized by high AOU, with values

9 reaching 59.3 µmol L^{-1}. In the South Aegean basin (Fig. 1), the AOU levels do not exceed 47.7

10 µmol L^{-1}. The CIW signature was also detected at about 250 m depth in the South Aegean station

11 from its low AOU (16.9 µmol L^{-1}), evidence of recent ventilation during the previous winter.

12   DOC ranged from 77 to 120 µmol C L^{-1} in surface waters where UDOM was collected

13 (Table 1; avg. ± sd = 93 ± 18 µmol C L^{-1}), and from 48 to 65 in subsurface waters (avg. ± sd = 54

14 ± 6 µmol C L^{-1}). A negative correlation was observed between AOU and DOC for all samples

15 with AOU > 0 collected during the POSEIDON cruise ($R^2 = 0.53$, $n = 33$, $p << 0.001$; Fig. 3).

16 Based on estimates of the slope of this relationship and a molar respiratory quotient of 106/154

17 (Anderson and Sarmiento, 1994), Arístegui et al. (2002) determined that DOC accounted for <

18 10% of AOU in deep open ocean waters. In this study, we observe a ΔDOC/ΔAOU value (± 95%

19 confidence interval) of -0.19 ± 0.12 for waters where AOU > 0 (Fig. 3). To correct for changes in

20 DOC due to mixing, potential temperature was included in this multiple regression analysis,

21 according to Doval and Hansell (2000). DOC removal in the EMS thus accounts for 27 ± 18% of

22 AOU and is higher than previous estimates for the global ocean (< 10%; Arístegui et al., 2002)

23 and consistent with that observed for specific water masses of the Mediterranean Sea (Santinelli

24 et al., 2010). This estimate is slightly higher than estimates of DOC respired during North

25 Atlantic Deep Water formation (7-29%, Carlson et al. 2010) and is more similar to estimates at

26 shallower depths in the open ocean (e.g., 15 to 41% at the BATS site; Hansell and Carlson 2001).

27 This estimate includes samples collected from a variety of water masses in the subsurface EMS,

28 thus yielding more variability than that reported for studies of ΔDOC/ΔAOU along isopycnals

29 (e.g., Doval and Hansel 2000). The mesopelagic and bathypelagic waters of the EMS are

30 relatively warm (> 13°) and DOC rich (48-65 µmol C L^{-1}) compared to open ocean basins, and

31 are thus likely to exhibit more efficient or extensive DOC respiration (Carlson et al. 2010).

32   Nutrient concentrations and picoplankton abundance and activity were also determined at

33 depths where seawater was collected for UDOM isolation (Table 2). Dissolved inorganic

34 nitrogen (DIN) and phosphorus (DIP) collected during the POSEIDON cruise exhibited profiles

1   typical for the ultra-oligotrophic EMS, with surface concentrations ranging from below detection

2   limits to 0.81 μmol L^{-1} and 0.05 μmol L^{-1}, respectively, and increasing to 4.8 μmol L^{-1} and 0.16

3   μmol L^{-1}, respectively, in subsurface waters (Table 2). The high subsurface DIN:DIP ratios (avg.

4   ± sd = 28 ± 4) agree with previous reports of the phosphorus-deficient EMS (Krom et al. 1992,

5   Krasakopoulou et al. 1999).

6   The mean (± sd) abundance of picoplankton was $4.3 ± 1.7 × 10^5$ cells mL^{-1} in the surface

7   and $8.3 ± 4.4 × 10^4$ cells mL^{-1} in subsurface waters. In general, at stations where UDOM was

8   collected *Bacteria* represented the bulk of picoplankton in both surface (65 ± 10%) and

9   subsurface (39 ± 10%) waters (data not shown). Picoplankton abundance estimated by flow

10   cytometry was well correlated with DOC (Fig. 4a, $R^2 = 0.67$, $n = 26$, $p \ll 0.001$). Some samples

11   from the subsurface depths (ranging from 100 to 250 m) of the S. Aegean were above the general

12   trend (circles). These outliers may be indicative of region-specific processes, such as the high

13   dust-deposition event that occurred in this area during the sampling period. Picoplankton

14   abundance was also well correlated with DOC at depths below 100m (Fig. 4b, $R^2 = 0.44$, $n = 18$,

15     $p < 0.005$). DOC was also well correlated with heterotrophic picoplankton activity (Fig. 4c, $R^2 = $

16   0.72, $n = 39$, $p \ll 0.001$). Fig. 4d is a plot of these variables below 100m. There was a

17   significant correlation at depths >300m ($R^2 = 0.27$, $n = 21$, $p < 0.02$), but samples at depths

18   between 100m and 300m plotted below this trend.

19   Picoplankton carbon biomass comprised < 0.8% of bulk DOC, confirming that changes

20   in picoplankton abundance alone cannot explain the observed variability in DOC. Sempéré et al.

21   (2002) showed similar relationships between DOC and bacterial production in the Northern

22   Aegean, attributing these trends to the enhancement of bacterial activity driven by input of DOC

23   from the Black Sea. The close association between DOC stocks and picoplankton abundance and

24   activity observed in this study is similar to those gradients found in estuarine and coastal aquatic

25   systems (e.g. Wetzel, 1992; Fernandes et al., 2008), but is rare for marine systems (e.g., Carlson

26   and Ducklow, 1995; Kaartokallio et al., 2007; H. Ducklow, pers. comm.). This tight coupling,

27   together with the relationship between AOU and DOC, imply that heterotrophic remineralization

28   processes exert a significant control on the cycling of DOC in these waters.

29

30   *3.2 UDOM Isolation and Correlations with AOU and the Picoplankton Community*

31

32   UDOM samples (n = 17) were concentrated with a spiral-wound filter of a nominal

33   MWCO of 500 Da; DOC retention efficiencies are reported in Table 1. This system retained 65%

34   of a 820 Da fluorescent compound (Alexa Fluor 594 dye) that was concentrated from 7L to 1.8L.

1   Fluorescence was intermittently detected in the permeate of the system, most notably during

2   ultrafiltration of the first 3L of solution (data not shown). The 500 Da cartridge filters processed

3   pre-filtered seawater at approximately 30 L h^{-1}, and retained on average (±SD) 49 ± 17% of DOC

4   in surface and subsurface seawater samples (Table 1). Amino acid analyses were performed on

5   aliquots of UDOM at this stage. Subsequently, UDOM samples were diafiltered to remove salts,

6   which also removed organic carbon and reduced the retention efficiency to an average (±SD) of

7   25 ± 12%. These samples were then lyophilized and used for monosaccharide and ^{1}H-NMR

8   characterization analyses. These analyses are discussed in further detail below.

9   The correlation between DOC and the picoplankton community was not paralleled by the

10   UDOC pool. Also, there was no correlation between UDOC and total DOC, or with AOU.

11   Together, these observations suggest that *bulk* UDOC is not representative of the component of

12   DOC that is coupled to the picoplankton community. While *bulk* UDOC was apparently unrelated

13   to either AOU or picoplankton proxies for remineralization, *specific components* of UDOC did

14   appear to be tightly coupled to both AOU and the microbial community (see below).

15   The variability in UDOC recovery reported in Table 1 (%DOC retained) is relatively high

16   compared to previous ultrafiltration studies in the marine environment (e.g., Guo et al., 1996;

17   Aluwihare et al., 1997; Benner et al. 1997). This result could be due to our use of a 500 Da

18   membrane for ultrafiltration; to the authors' knowledge this study provides the first reports of the

19   chemical characteristics of this fraction of DOM. As such, we are unable to determine if high

20   variability in UDOC recovery is an artifact of sampling procedures or natural variability. We

21   considered the possibility that UDOC recovery influenced the variability observed for each

22   UDOM chemical composition parameter determined in this study. Indeed, one may expect that

23   variability in the percentage of DOC that is > 500 Da, whether derived naturally or from sampling

24   procedures, could yield substantial variability in the concentration and distribution of amino acids

25   and monosaccharides in UDOM. Despite this concern, only the heteroatom ^{1}H-NMR resonances

26   showed a slightly significant correlation with variability in UDOC recovery (r = -0.55, p = 0.05).

27   Other correlations with UDOC recovery, or lack thereof, are presented throughout the

28   manuscript. If insufficient sampling protocols resulted in variability in UDOC recovery and

29   altered the chemical composition between samples, the strong correlations between UDOC-

30   specific chemical composition measurements and independent measurements of other site-

31   specific parameters reported below are a remarkable coincidence.

32   To further examine the UDOM chemical composition of the various water masses, we

33   determined ^{1}H-NMR spectra as well as amino acid and monosaccharide concentrations and

34   relative mole distributions. The data were sorted according to the AOU value of the

1   corresponding water masses to assess the correlation between UDOM chemical composition and

2   AOU (Tables 3 and 4). Comparisons of UDOM composition in this study are drawn between

3   samples that were 1) isolated during the POSEIDON cruise and analyzed prior to diafiltration for

4   amino acid characterization, or 2) isolated during either the POSEIDON or SESAME cruises and

5   analyzed after diafiltration for carbohydrate and ^{1}H-NMR characterization. While these data

6   likely represent different fractions of bulk DOM, no comparisons are drawn between these

7   fractions unless otherwise noted.

8

9   *3.3 UDOM ^{1}H-NMR Characterization*

10

11   Selected ^{1}H-NMR spectra are shown in Fig. 5 and the relative contribution of aliphatic

12   (0.5 to 1.8 ppm), alpha-substituted (1.8 to 3.2 ppm), and heteroatom-substituted resonances (3.2

13   to 4.6 ppm) in all UDOM samples are reported in Table 3 alongside carbohydrate data. ^{1}H-NMR

14   spectra were dominated by characteristic aliphatic, alpha-substituted (acetate), and heteroatom-

15   substituted resonances, and trends in the relative abundance of these resonances were similar to

16   previous reports (e.g., Aluwihare et al., 2002). In general, UDOM from higher AOU waters (i.e.,

17   subsurface UDOM) exhibited ^{1}H-NMR spectra with proton abundance evenly distributed as

18   broad peaks among all resonances, while ^{1}H-NMR spectra of UDOM isolated in low AOU waters

19   were dominated by the heteroatom-substituted (likely carbohydrate) resonances. Aliphatic and

20   alpha-substituted resonances were significantly correlated with AOU ($r = 0.73$ and 0.92,

21   respectively, $p < 0.005$; Table 3). Heteroatom-substituted resonances were significantly and

22   inversely correlated with AOU ($r = -0.85$, $p < 0.001$). UDOM collected from the N. Aegean

23   basin (1000m) exhibited a ^{1}H-NMR spectrum similar to that observed for surface samples

24   dominated by heteroatom-substituted resonances (Fig. 5, Table 3). This anomalous sample was

25   excluded from the UDOM comparisons in this section and from those discussed below, unless

26   otherwise noted.

27

28   *3.4 UDOM Carbohydrate Composition*

29

30   Monosaccharide abundances and distributions in UDOM are reported in Table 3 and are

31   sorted according to the AOU value of the corresponding water mass. DCNS ranged from 0.4 to

32   3.8 µmol C L^{-1}, representing 2 to 24% of UDOC (Table 3); these carbohydrate yields are

33   consistent with previous reports (e.g., Aluwihare et al., 2002; Benner, 2002). Both DCNS and

34   %NS-UDOC were correlated with ^{1}H-NMR aliphatic, alpha-substituted, and hetero-atom

1 substituted resonances (r = -0.69, -0.61, and 0.67, respectively; p < 0.05), and generally showed

2 increased concentrations in surface waters but were not significantly correlated with AOU or

3 picoplankton activity. Relative mole percentages (mol %) of galactose (avg. ± sd = 26.4 ± 3.4%),

4 glucose (20.4 ± 1.9%), and mannose (17.2 ±1.7%) were consistently high in all UDOM samples;

5 this latter observation is unique to this sample set as mannose typically exhibits lower relative

6 mol % in UDOM (e.g., 10 to 16 %; McCarthy et al., 1996; Aluwihare et al., 2002). In general,

7 UDOM isolated for this study exhibited a monosaccharide composition consistent with previous

8 UDOM reports even though it likely includes relatively more of the LMW pool of DOM

9   AOU was significantly correlated with mol % of glucose (r = 0.54, p < 0.05) and was

10 significantly and inversely correlated with mol % of galactose (r = -0.76, p < 0.005). No other

11 monosaccharide mol % was correlated with AOU. The significant correlations observed for

12 glucose and galactose with AOU imply that these monosaccharides vary inversely during the

13 apparent degradation of semi-labile UDOM, or other processes that contribute to increase the

14 AOU of a water mass. These observations are similar to previous reports of galactose and glucose

15 variability in seawater (e.g., McCarthy et al., 1996; Skoog and Benner, 1997; Amon and Benner,

16 2003; Goldberg et al., 2009).

17   Similar to previous studies, carbohydrates were a relatively small fraction of bulk DOC

18 (< 4 μmol C L^{-1}) and thus represented only a small fraction of the change in DOC or AOU

19 between surface and deep waters. Thus, the observed correlations between monosaccharide

20 distributions and AOU may not be a direct representation of the removal semi-labile TOC in

21 subsurface waters. That is, the standing stock of non-carbohydrate UDOC removed as AOU

22 increases far exceeds that of carbohydrate UDOC, and changes in monosaccharide distributions

23 may be complementary to this flux. Rather than representing the effects of selective preservation

24 or consumption of a semi-labile carbohydrate component, monosaccharide distributions may

25 reflect transient fluxes of monosaccharides in UDOM that become more important in the deep

26 ocean.

27

28 *3.5 UDOM Amino acid Composition*

29

30   Amino acid concentrations and mole distributions were determined for 8 UDOM samples

31 before diafiltration; samples were sorted according to AOU values and data are shown in Table 4.

32 In general, the UDOM isolated in this study represents a greater fraction of bulk DOM than

33 previous UDOM reports and the composition of this pool may exhibit signatures more closely

34 related to LMW DOM than previous UDOM composition studies. For example, Kaiser and

17

1   Benner (2009) report lower yields of amino acids and relatively depleted abundances of

2   hydrophobic amino acids in LMW DOM compared to HMW DOM. In this study, the

3   concentrations of DCAA ranged from 51 to 158 nmol L^{-1} (188 to 581 nmol C L^{-1}) in surface and

4   subsurface waters. Glycine was by far the most abundant amino acid in all UDOM samples,

5   representing $35.0 \pm 1.9\%$ (avg. $\pm$ sd) of all amino acids, followed by aspartic acid ($12.4 \pm 1.1\%$),

6   glutamic acid (9.0 ± 0.7), and alanine (8.1 ± 0.6). Amino acids in UDOM represented $41 \pm 11\%$

7   of amino acids measured in bulk seawater samples (thus a significant amount is present in the

8   HMW fraction); and bulk seawater samples showed similar mole distributions, except for

9   significantly higher relative abundances of alanine ($14.3 \pm 3.5\%$, $p < 0.001$) and serine ($7.4 \pm$

10   3.9%, $p < 0.005$, data not shown). Several amino acids were below the detection limit in bulk

11   seawater samples and were not considered in mole distribution comparisons. The range in DCAA

12   observed in this study is lower than that reported for UDOM in the open ocean (178 to 278 nmol

13   L^{-1}; McCarthy et al. 1996). However, the relative distributions (mol%) of amino acids in UDOM

14   agree with previous reports, as does the fraction of amino acids in UDOM relative to the total

15   pool of amino acids determined in bulk seawater samples (Aluwihare and Meador 2008, and

16   references therein). The amino acid carbon contribution to UDOC (%AA-UDOC) ranged from

17   0.83 to 1.61% and was lower than previous reports (~3 to 6%; Benner et al., 2002; Aluwihare and

18   Meador, 2008); the error of this value was < 0.03% for all samples.

19   The average ($\pm$ sd) enantiomeric ratios (D/L) of aspartic acid (0.39 ± 0.11) and alanine

20   (0.56 ± 0.11) were similar to the averages in the open ocean (0.42 and 0.49, respectively; Pérez et

21   al., 2003) and in UDOM (0.37 and 0.50, respectively; McCarthy et al., 1998). The D/L ratios for

22   serine (0.60 ± 0.17) and glutamic acid (0.30 ± 0.05) appear to be enriched in the D-enantiomer

23   compared to previous reports (0.09 and 0.15, respectively; Pérez et al., 2003). McCarthy et al.

24   (1998) report a D/L ratio for tyrosine of 0.10, which was not much higher than the blank reported

25   for that study, and lower than observed in this study (0.17 ± 0.05). The enantiomeric amino acid

26   ratios determined in this study were corrected for hydrolysis-related racemization according to

27   Kaiser and Benner (2005), whereas the previous reports serving as comparisons did not apply this

28   correction. Our uncorrected enantiomeric data were not significantly different from the corrected

29   data, maintaining the same relationship as the comparisons noted above.

30   The UDOM sample collected in the deep N. Aegean basin (1000m) was not included in

31   the computations above or those in the proceeding amino acid discussion. The composition of

32   this deep ocean sample was remarkably similar to samples collected in the surface ocean,

33   particularly in regard to its ^{1}H-NMR spectra (Fig. 5) and low D-amino acid content (Table 4).

34   This sample also exhibited the lowest UDOC (21 μM ultrafiltered, 5 μM diafiltered; Table 1).

1 These characteristics may result from the unique ventilation patterns of the N. Aegean basin,

2 where the rapid deep water formation and reduced mixing presumably could have affected the

3 chemical composition of UDOM. Additionally, prior to deep water formation, these waters likely

4 contained alloctonous inputs of DOM from the Black Sea that may differ in chemical

5 composition from that produced in the EMS. These findings provide additional evidence that

6 North Aegean deep waters differ from the rest of the EMS deep water masses due to a long

7 stagnation period from 1994 to at least 2007 (our sampling year), during which there has been

8 low or no ventilation (Zervakis et al., 2003; Zervakis and Krasakopoulou, unpublished data).

9

10 *3.5.1. Amino Acids and AOU*

11   Assessing the correlation between AOU and the amino acid composition of UDOM

12 allowed us to examine the chemical transformations of DOM that may accompany increases in

13 AOU, which seemingly represents the degradation of semi-labile DOC. Significant correlations

14 between AOU and %AA-UDOC and mole distributions are shown in bold in Table 3. AOU and

15 %AA-UDOC were significantly and inversely correlated (r = -0.98, p < 0.001). DCAA showed

16 a similar but less significant correlation with AOU (r = -0.74, p = 0.063). It thus appears that

17 %AA-UDOC integrates a multitude of processes that are coupled to AOU but that are not

18 represented by DCAA alone. While there was a strong correlation between %AA-UDOC and

19 AOU (Fig. 6), amino acid carbon normalized to *bulk* DOC shows no correlation with AOU (r =

20 0.16). The amino acid signature that accompanies changes in AOU is thus only evident in the

21 dynamics of UDOC, and presumably, associated with the HMW fraction of bulk DOC. Given

22 that the ultrafiltration sampling procedures, which may have artificially altered UDOC recovery,

23 did not affect AOU measurements, the correlation between AOU and %AA-UDOC provides

24 convincing evidence that the range in UDOC recovery reported in Table 1 records natural

25 variability.

26   The increase in %AA-UDOC in low AOU waters is likely due to local production by

27 marine autotrophs in the surface ocean (e.g., Hubberton et al., 1994), an amino acid source that is

28 absent from high AOU waters in the subsurface ocean. Table 4 also reveals that UDOM mole

29 percentages of D-asp, D-glu, and gly were significantly correlated with AOU (r = 0.89, 0.84, and

30 0.80, respectively; p < 0.05), and ser, thr/his, and tyr were significantly and inversely correlated

31 with AOU (r = -0.90, -0.89, and -0.95, respectively; p < 0.01). Some of these significant

32 differences were observed in previous reports of amino acid distributions in the marine

33 environment, which have generally noted increased concentrations of alanine and glycine, and

34 decreased concentrations of hydrophobic amino acids (e.g., leucine, phenylalanine, valine) in

1   "more degraded" DOM (e.g., Yamashita and Tanoue, 2003).   In this study, the sum of the total

2   carbon-normalized D to L-enantiomeric amino acids in UDOM (Σ-D/L) ranged from 0.23 to 0.44.

3   Σ-D/L of UDOM was significantly correlated with AOU ($r = 0.77$, $p < 0.05$) and was primarily

4   driven by changes in D-asp and D-glu (Table 4). These amino acids also appeared to increase

5   with depth; this observation contrasts that observed by McCarthy et al. (1998) in the North

6   Atlantic and Pacific basins and may be due to the higher recovery of UDOM examined in this

7   study or differences in the subsurface regions of the EMS versus the open ocean.. The dynamics

8   of D-amino acids are further discussed below

9   In this study, amino acids accounted for less than 2% of UDOC and less than 0.2% of

10   bulk DOC (< 0.6 μmol C L^{-1}). As above for carbohydrates in seawater, the addition and removal

11   of the < 0.6 μmol C L^{-1} fraction of amino acid carbon cannot account for the large changes

12   observed in AOU. Thus, the correlation between amino acid distributions and AOU may not

13   directly reflect which of the amino acids are preferably removed or preserved as semi-labile

14   UDOM is degraded, but may represent transient fluxes of amino acids in UDOM that vary with

15   increasing AOU. For example, Pérez et al. (2003) speculated that the shift in the bacterial uptake

16   ratios of D/L-amino acids from the surface to the mesopelagic zone of the N. Atlantic may reflect

17   a shift in the production of bioavailable D/L-amino acids.

18

19   *3.5.2. Amino Acids and picoplankton*

20

21   Similar to trends observed with AOU, picoplankton community parameters were also

22   significantly correlated with %AA-UDOC (Fig. 7) and were not correlated with DCAA. In order

23   to assess the relationships between amino acid and picoplankton parameters, it is necessary to

24   consider the inherent intracellular protein component that comprises a substantial portion of the

25   microbial biomass. The measured carbon concentrations of amino acids in UDOM and those

26   calculated for the picoplankton community (assuming 2×10^{-14} g C $cell^{-1}$, an overestimate for the

27   purpose of this comparison; Fukuda et al., 1998) are of the same order of magnitude ($\sim 10^{-7}$ mol

28   C L^{-1}); however, there was no significant correlation between these parameters. These

29   measurements thus appear to be exclusive, and the reported DCAA concentrations (in UDOM)

30   are in fact measures of amino acids in the dissolved pool and do not include picoplankton

31   biomass. Therefore, the correlations observed between amino acid and microbial parameters in

32   Fig. 7 reflect the distinct variability of UDOM composition or the picoplankton community.

33   Estimates of %AA-UDOC appear to be significantly correlated with both picoplankton

34   abundance and cell specific picoplankton activity (Fig. 7a, b; $R^2 > 0.89$, $p < 0.002$; note that the y-

1   axis is a log scale). The relationship shown in Fig. 7a suggests that the proportion of amino acids

2   in UDOC, while < 2% of UDOC, is tightly coupled to picoplankton abundance. Because count-

3   estimated picoplankton abundance in deep waters may include dormant cells, the significant

4   relationship between %AA-UDOC and picoplankton activity (Fig. 7b) provides more convincing

5   evidence that amino acids in UDOM are coupled to the picoplankton community. This

6   relationship also applies when considering only the metabolically slow dark ocean regions (i.e.,

7   those samples with %AA-UDOC < 1.3% in Fig. 7). DCAA was not correlated with picoplankton

8   activity or abundance, or with AOU (Fig. 6).

9   Picoplankton activity and AOU are clearly associated with different timescales of

10   turnover of organic matter (hours versus years), yet are related as increases in AOU record the

11   cumulative effects of heterotrophic activity, and this metabolic activity becomes energetically

12   constrained and decreases as a water mass ages (e.g., Hoehler, 2004). Fig. 6 and Fig. 7 show that

13   %AA-UDOC is strongly correlated with both AOU and picoplankton activity, but it is unclear

14   whether: 1) %AA-UDOC mimics the relationship between DOC and AOU (Fig. 3) and also

15   records the accumulative effects of heterotrophic activity over long timescales (i.e., more

16   bioavailable amino acid components are removed and refractory components remain); or 2)

17   changes in %AA-UDOC are manifested more rapidly, in equilibrium with reduced picoplankton

18   activity.

19   The latter explanation is supported by the lack of correlation between DCAA and AOU

20   or picoplankton activity (Figs. 6 and 7). If the former explanation was valid we would expect that

21   DCAA would track AOU, similar to bulk DOC (Fig. 3), as the bioavailable components of

22   UDOM set in the surface ocean are gradually removed. Also, the magnitude of the stocks of

23   picoplankton and amino acids ($\sim 10^{-7}$ mol C L^{-1}) are similar, whereas that required to account for

24   the AOU signal is much larger ($\sim 10^{-5}$ mol C L^{-1}). Further investigation of the co-variability

25   between individual amino acid mole distributions and the picoplankton community are

26   considered below.

27

28   *3.6 Principal component analysis (PCA) of UDOM*

29

30   Several indices assess the degree of degradation of organic matter; these are based on

31   trends in monomer composition (e.g., Dauwe et al., 1999; Amon et al., 2001; Amon and Benner

32   2003) or make use of biomarkers to estimate the contribution of bacteria to DOM (e.g., McCarthy

33   et al., 1998; Kaiser and Benner, 2008). These strategies interpret the composition of DOM in the

34   parlance of amino acid or monosaccharide composition. AOU is a more direct proxy for

21

1 remineralization of organic matter and is correlated to DOC stocks (Fig. 3); we assessed UDOM

2 molecular level composition as it relates to this signal above (Tables 3 and 4). PCA identifies the

3 axes that capture the greatest amount of variability within the sample set and thus presents an

4 alternative framework to compare variability in UDOM composition. We used PCA to examine

5 the variability in both amino acid and monosaccharide distributions in UDOM, similarly to

6 Dauwe et al. (1999) who characterized diagenetic trends of sedimentary organic matter. However,

7 the PCA analysis in this study considered several biogeochemical proxies, in addition to those

8 related to diagenesis, in order to establish correlations with the axes that explain the majority of

9 variability in molecular level composition.

10 PC1 and PC2 accounted for 48% and 31% of the variability in amino acid mol %, and

11 36% and 25% of monosaccharide mol % variability, respectively. Factor loadings for PC1 and

12 PC2 of individual amino acids and monosaccharides are plotted in Fig. 8; amino acids or

13 monosaccharides that cluster together vary similarly among UDOM samples. Also, PC1 and PC2

14 scores were generated for individual UDOM samples for both the amino acid and

15 monosaccharide PCA (data not shown); these scores sort UDOM samples along the first and

16 second principal component axes of compositional variability. PC scores were compared to

17 additional biogeochemical data determined for each UDOM sample or sampling station.

18 Significant correlations are reported in Table 5 and are sorted according to parameters that

19 generally increase or decrease with depth. Thus, the information provided by PCA allowed us to

20 distinguish the covariability between individual amino acids and monosaccharides within UDOM

21 and the covariability between UDOM molecular composition and multiple site-specific

22 parameters (in addition to the AOU comparisons above). The UDOM sample collected in the

23 deep N. Aegean basin (1000m) was not included in PCA for the reasons described above.

24

25 *3.6.1. Amino Acid PCA*

26

27 The PC1 and PC2 loadings derived for each amino acid were used to sort amino acids

28 into clusters, such that amino acids with similarly high loadings for either the PC1 or PC2 axis

29 were grouped together (Fig 8a). Amino acid clusters are identified as:

30 Cluster I – arginine, L-aspartic acid, leucine, and valine

31 Cluster II - L-alanine, L-serine, L-tyrosine, and the threonine and histidine peak

32 Cluster III - D-serine and D-tyrosine

33 Cluster IV - D-alanine, D-aspartic acid, D-glutamic acid, and glycine

22

1   Phenylalanine and L-glutamic acid were not sorted into groups because the PC1 and PC2

2   loadings for these amino acids were relatively low.

3   This amino acid PCA analysis is similar to that reported by Yamashita and Tanoue

4   (2003) for amino acids in coastal and open ocean DOM. Clusters II and IV exhibit high but

5   opposite loadings for PC1. Clusters I and III have high and opposite loadings for PC2. These data

6   indicate that variability of amino acids clusters II and IV are inversely proportional and best

7   described by PC1, and any parameters correlated with PC1 are also likely correlated with the

8   distribution of these amino acids. Similarly, parameters that are correlated with PC2 are likely

9   correlated with amino acids in clusters I and III. The trends observed in this study are difficult to

10 compare to those observed in Yamashita and Tanoue (2003) because we did not measure the

11 same suite of amino acids (e.g., D-enantiomers are not reported in their study); however, these

12 authors report similar relationships between glycine and the hydrophobic amino acids valine and

13 leucine for PC1, as well as the similarly high loadings for arginine and L-aspartic acid for PC2.

14   The first principal component of variability in amino acid distribution (i.e., PC1) was

15 significantly correlated with %AA-UDOC ($r = 0.96$, $p < 0.001$), but was not significantly

16 correlated with DCAA or with %DOC retained by ultrafiltration. From this observation we can

17 deduce that variability in amino acid mol % distribution was 1) more significantly coupled to the

18 protein component of UDOM and not bulk amino acid concentrations in seawater; and 2) not an

19 artifact of sampling procedures that may have altered retention of UDOC. A similar correlation

20 with PC1 and %AA-UDOC was observed by Amon et al. (2001) and Yamashita and Tanoue

21 (2003), which led these authors to suggest that degradation was the principal component driving

22 the variability within their datasets. PC1 was also correlated with picoplankton abundance and

23 activity ($r = 0.93$ and 0.89, respectively; $p < 0.005$), and inversely correlated with AOU ($r = -$

24 0.90, $p < 0.01$) and Σ-D/L ($r = -0.83$, $p < 0.02$; Table 5). PC1 thus captures the variability that

25 was addressed in sections 3.5.1 and 3.5.2 above, which used a more obtuse analysis of amino acid

26 distributions, and indicates that D- amino acids in cluster IV are among the most variable amino

27 acids in UDOM.

28   PC1 of amino acid mol % distribution was also significantly correlated with other

29 UDOM composition measurements, including aliphatic, alpha-substituted, and heteroatom-

30 substituted regions of UDOM ^{1}H-NMR spectra ($r = -0.91$, -0.97, and 0.98, respectively; $p <$

31 0.005) and several other parameters that are associated with water mass age or depth-related

32 trends in the water column (Table 5). This observation indicates that changes in UDOM [1]H-

33 NMR spectra are accompanied by changes in the mol % signature of amino acids in UDOM; in

34 particular, those amino acids with high absolute loadings for PC1 (i.e., clusters II and IV, Fig.

8A). The amino acids D-asx, D-glx, gly, and D-ala (cluster V, with low PC1 loadings) are
relatively more abundant in UDOM with ^{1}H-NMR spectra exhibiting higher aliphatic and alpha-
substituted resonances; ala, leu, val, phe, and asx (cluster II, with high PC1 loadings) are more
abundant in UDOM with ^{1}H-NMR spectra exhibiting higher heteroatom substituted resonances.
Again, amino acids are a small fraction of UDOC and these amino acids have similar abundances
of aliphatic, alpha-substituted, and heteroatom substituted protons (if anything the cluster II
amino acids would have relatively more aliphatic protons); therefore the amino acid distributions
are not directly driving the observed variability in ^{1}H-NMR spectra. Variability in amino acid mol
% and ^{1}H-NMR resonances do appear to be impacted by the same, unidentified, principal
component however. As noted above, the diafiltered sample used to determine ^{1}H-NMR spectra
contained a smaller portion of the total DOC pool than that used for amino acid measurements,
and it is possible that the DOM lost during diafiltration (in preparation for ^{1}H-NMR analysis) was
enriched in cluster IV amino acids as well as aliphatic and alpha-substituted resonances, or
relatively depleted in cluster II amino acids and heteroatom-substituted resonances. Kaiser and
Benner (2009) reported that open ocean LMW DOM exhibited lower abundances of hydrophobic
amino acids and total neutral sugars than the HMW counterpart, and this may explain the
correlation reported in Table 5.

PC1 has been interpreted as an index of degradation (Dauwe et al., 1999; Amon et al.,
2001; Yamashita and Tanoue, 2003; Kaiser and Benner, 2009). But as the PCA derived in this
study was correlated with both the long-term degradation signal represented by AOU, and more
rapid signals related to picoplankton activity, the PCA results do not favor either hypothesis that
attempts to explain variability in %AA-UDOC or amino acid distribution noted above (e.g.,
selective degradation versus alternative metabolism). While D- amino acids in cluster IV are
considered more refractory and the observed positive correlation with AOU agrees with this
prediction, D-amino acids are also known to be produced and metabolized by marine
picoplankton in the deep ocean (Pérez et al., 2003; Teira et al., 2006; Kaiser and Benner, 2008;
Varela et al., 2008), and the variability captured by PC1 may derive from the relative enhanced
contribution of these organisms to production in the deep ocean.

Kaiser and Benner (2008) suggested the use of relative abundances of D- amino acids (D-
AA) to TOC as a biomarker for bacteria-derived DOM. We estimated the contribution of bacteria
to TOC in the EMS using yields determined in this study and end-member estimates of D- AA
yields in DOM produced by bacteria in culture (0.29, 0.20, and 0.42 nmol D-AA µmol TOC[-1] for
D-Asp, D-Glu, and D-Ala, respectively; Kaiser and Benner, 2008) using the equation:

$$\%\text{Bacteria-derived DOM} = 100 \times ([\text{D-AA}]/[\text{TOC}])_{sample} / ([\text{D-AA}]/[\text{TOC}])_{culture}$$

Average values ranged from 8 to 29% of TOC for all UDOM samples (including the deep N. Aegean, Fig. 9); these values are similar to those reported throughout the water column and at the BATS and HOT sites (Kaiser and Benner, 2008), but there were large standard deviations in estimates generated by the three D-AA biomarkers (coefficient of variation ranged from 16 to 34%). Bacteria-derived DOM was not correlated with PC1 (and thus not with AOU, picoplankton abundance, or activity). This was unexpected, considering that the variability of the D-AA biomarkers used for this calculation appear to drive PC1, and may be a result of comparing amino acid signatures (described by the PCA) with absolute amino acid concentrations (used for this calculation). The lack of correlation of bacteria-derived DOM with PC1 suggests that there was no significant accumulation of the amino acid component of this flux of DOM. Bacteria-derived DOM in subsurface samples ($n = 6$) was correlated with PC3 however ($r = 0.87$, $p < 0.05$), which explained 9% of amino acid distribution variability and was also correlated with UDOC ($r = 0.82$, $p < 0.05$).

Estimates of bacteria-derived DOM rely on D-AA yields in DOM produced by bacteria cultures; coefficients of variation range from 12 to 43% (Kaiser and Benner 2008) and must thus be interpreted with caution. As discussed above, the amino acid component of UDOC was tightly coupled to picoplankton activity whereas that of bulk DOC was not (Fig. 4); therefore, D-AA may serve as a more accurate biomarker index of bacteria-derived DOM contribution if calculated normalized to UDOC rather than TOC. Further assessment of this parameter will require a larger collection of subsurface UDOM samples and a more thorough understanding of the production of D-AA by marine picoplankton in culture.

PC2 also described a substantial portion of amino acid mole % variability (31%) but was not correlated with any parameters measured in this study; as such, we are unable to interpret the variability associated with this axis or the fluxes that affect the amino acids in cluster I and III. The primary controls of the distribution of these amino acids appear to differ from clusters II and IV and may result in different residence times of these amino acids in seawater. Martín-Cuadrado et al. (2007) found that genes for the metabolism of glycine, serine, and threonine (from clusters II and IV) were among the most frequent observed in picoplankton collected from the deep Ionian Sea (second only to ABC transporters). Genes for metabolism of cluster I amino acids were also present but ~30% less frequent. Genes for carbohydrate biosynthesis and metabolism genes were almost an order of magnitude less frequent than those for amino acids.

3.6.2. Monosaccharide PCA

PC1 and PC2 accounted for 36% and 25%, respectively, of the variability in monosaccharide distributions. The biplot of PC1 and PC2 loadings of individual monosaccharides were more scattered than those for amino acids (Fig. 8b) and no clusters were identifiable. Galactose and the methyl-sugars (i.e., rhamnose and fucose, also deoxy-sugars) exhibited the greatest positive and negative loadings for PC1, respectively; xylose and mannose had the greatest positive and negative loadings for PC2, respectively. While these monosaccharides exhibited the highest absolute factor loading values for PC1 and PC2, several monosaccharides demonstrated relatively large factor loadings in both dimensions (Fig. 8b) and cannot be ignored when considering the variability captured by PCA.

No site-specific parameters measured in this study were immediately identified as correlated with PC1 scores of UDOM monosaccharide mol % (i.e., $p > 0.05$ for all comparisons), indicating that the primary mechanism that determines monosaccharide distributions is extremely dynamic and seemingly unrelated to other site-specific parameters determined in this study. The carbohydrate component of DOM is considered to be reactive given the large changes in carbohydrate abundance between surface and deep DOM (e.g., Repeta and Aluwihare, 2006). Even though glucose and galactose mol % were significantly correlated with AOU when considered individually (Table 3), and these monosaccharides exhibit opposite loadings for PC1 (Fig. 8b), we do not observe a significant correlation between PC1 and AOU. The highly positive PC1 factor loadings for methyl-sugars (Fig. 8b) reveal that the distributions of these monosaccharides (which were not correlated to AOU; Table 3) are an important source of variability in these UDOM samples. Biogeochemical fluxes related to the turnover of methyl-sugars may thus alter monosaccharide distributions and suppress the remineralization trends that are related to processes driving variability in galactose, glucose, and AOU. The D-AA biomarker index for bacteria-derived DOM (see previous section; Kaiser and Benner, 2008) was significantly correlated with PC1 of monosaccharide distribution ($r = 0.87$, $p < 0.05$). Thus, while the D-AA based estimation of DOM contributed by bacteria did not appear to be associated with amino acid PCA, this contribution may be represented in the monosaccharide component of DOM and may represent the alternative flux associated with mol % of methyl-sugars.

Similarly to PC1 of amino acid distributions, several parameters were correlated with PC2 scores (Table 5). %NS-UDOC and DOC were significantly correlated with PC2 ($r = 0.60$, and 0.77, respectively; $p < 0.05$). ^{1}H-NMR resonances were also well correlated with PC2 ($r = -$0.85, -0.83, and 0.85 for [1]H-aliphatic, alpha-subs, and hetero-subs resonances, respectively, $p <$

1   0.005; Table 5). DCAA also showed a strong correlation with PC2 ($r = 0.96$, $p < 0.005$). Here

2   we observe another correlation between the two different fractions of UDOM (diafiltered versus

3   non-diafiltered) and this correlation may result from the losses during diafiltration. % DOC

4   retention showed no significant correlations with any PC derived for monosaccharide distribution

5   (Table 5), again suggesting that potential variability introduced as a result of sampling procedures

6   had no effect on variability of monosaccharide distributions. Additional correlations with PC2

7   include salinity, σ_θ, and AOU; these relationships are driven by surface or low-salinity end-

8   members and may not identify a continuous trend. In summary, correlations reported for PC2 of

9   monosaccharides represent both depth-related and composition-related parameters, and these

10   appear to vary with relative abundances of galactose, xylose, and fucose, and inversely with

11   glucose, mannose, arabinose, and rhamnose.

12

13   **4. Conclusions**

14

15   UDOM sampled from a variety of depths in the EMS targeted spatially distinct surface

16   waters as well as subsurface water masses that have been subducted below the euphotic zone for

17   different periods of time, thus exhibiting a range in AOU values. A negative correlation between

18   DOC and AOU observed in this study indicates that remineralization of semi-labile DOC can

19   account for $27 \pm 18\%$ of oxygen consumption in the subsurface EMS (Fig. 3). This is higher than

20   previous reports in the bathypelagic open ocean waters (i.e., < 10%; Hansell, 2002; Arístgui et al.

21   2002) and consistent with new reports for the Mediterranean Sea (Santinelli et al., 2010). DOC

22   exported from surface waters thus serves as a more important substrate for carbon respiration in

23   the warm (> 13ºC), deep waters of the EMS. DOC values were also closely associated with

24   picoplankton abundance and activity (Fig. 4), similar to relationships observed in estuarine

25   systems (e.g., Wetzel 1992, Fernandes et al. 2008) but rare for the open ocean (e.g., Carlson and

26   Ducklow, 1995; Kaartokallio et al., 2007).

27   While UDOM amino acids are a small component of DOC in the EMS (avg. $\pm$ SD = 0.33

28    $\pm$ 0.14 µmol C L^{-1}), we observed strong correlations between the relative amino acid component

29   of UDOM (%AA-UDOC) and AOU and picoplankton activity in water masses of the EMS ($p <$

30   0.002), but no correlation with DCAA (Figs. 6 and 7). These are strikingly significant

31   correlations between independent measures of the amino acid composition of UDOM and the

32   picoplankton community. The strong correlations observed in Fig. 6 and 7 indicate direct

33   connections between the amino acid component of UDOC and picoplankton carbon pools in

34   seawater, and may thus represent controls on the equilibrium between microbial assemblages and

1   DOM within the microbial loop. In addition, amino acid and monosaccharide distributions, as

2   well as ^{1}H-NMR spectra were significantly correlated with AOU (Tables 3 and 4). These trends

3   did not extend to the UDOM sample collected in the deep N. Aegean basin, which exhibited low

4   DOC and amino acid abundances, but a ^{1}H-NMR spectrum and amino acid and monosaccharide

5   mole distribution patterns similar to that found in the surface ocean (Fig. 5, Tables 3 and 4).

6   PCA revealed that the principal component of variability of amino acid distributions (i.e.,

7   PC1, explaining 48% of variability) was well correlated with %AA-UDOC and picoplankton

8   activity but inversely correlated with AOU. PC1 was also correlated with several other site-

9   specific parameters (Table 5). The PC1 axis captured the mole % variability of two inversely-

10   correlated clusters of amino acids: alanine, serine, tyrosine, and threonine/histidine (cluster II)

11   and D-alanine, D-aspartic acid, D-glutamic acid, and glycine (cluster IV; Fig. 8a), with cluster II

12   amino acids being relatively more enriched in UDOM with high %AA-UDOC and sampled from

13   regions with higher picoplankton activity and lower AOU. We were unable to determine if these

14   signatures were driven by 1) remineralization processes associated with semi-labile DOM that

15   was exported from the surface ocean, which occur over relatively long timescales, or 2) more

16   rapid DOM production and remineralization processes driven by local picoplankton communities

17   that also change with depth (e.g., De Corte et al. 2009). D- amino acid concentrations were used

18   as quantitative biomarkers to estimate the % of TOC contributed by bacteria (according to Kaiser

19   and Benner, 2008). This analysis suggested that bacteria produced 8-29% of DOM in samples

20   collected from the surface to 4350 m in the E. Mediterranean, but this parameter was not

21   correlated with PC1 of amino acid distributions. The flux of DOM produced by bacteria thus

22   does not appear to have accumulated or contributed significantly to the observed variability in

23   amino acid signatures. This observation, together with the significant correlation observed

24   between AOU and PC1, argue for the construction of amino acid distributions by remineralization

25   processes that occur over long timescales. However, the strong correlation between %AA-UDOC

26   and picoplankton activity, which is representative of carbon turnover on a much faster timescale,

27   suggests that more rapid and transient remineralization or alternative production signatures may

28   also be associated with increasing AOU. Together, these observations imply that the principal

29   component of variability in amino acid distributions is not well-defined and will require more

30   extensive study to be categorically assigned as an index of "degradation" or as an alternative

31   biogeochemical flux. This conclusion is consistent with similar analyses in the open ocean

32   (Meador, 2008; Kaiser and Benner, 2009).

33   Monosaccharide distributions appeared to be more dynamic, as PC1 (explaining 36% of

34   variability) was uncorrelated with most site-specific parameters and it was PC2 (explaining 25%

of variability) that showed correlations with %NS-UDOC, DOC, and other site-specific parameters (Table 5). Mole % of galactose and glucose were significantly correlated with AOU, similar to previous reports (McCarthy et al., 1996; Skoog and Benner, 1997; Amon and Benner, 2003; Goldberg et al., 2009), but the AOU signal was not strongly associated with PC1 or PC2. Fluxes associated with AOU thus do not appear to significantly influence monosaccharide distributions. PC1 was correlated with estimates of bacteria-derived DOM however, indicating that the flux of carbohydrates produced by bacteria may accumulate more significantly than that of proteins.

These collaborative analyses have begun to elucidate key relationships that connect DOM chemical characterization to heterotrophic metabolism and marine biogeochemical cycles. The chemical characterization of DOM in the EMS provided by this study represents the first such data for this region, and the enhanced respiration of DOC in the relatively warm "twilight" zone of the EMS was advantageous for establishing explicit correlations in DOM cycling, thus advocating for additional investigations of DOM and microbial composition dynamics in this unique region. Advancements in interpreting UDOM composition signals will rely, in part, on detailed studies targeting metabolism of the key amino acids and monosaccharides identified by this and other studies, and also on information provided by the intact macromolecules from which these signals were derived.

1   in the preparation of this manuscript. This work was performed within the 'Network of

2   Excellence' EurOceans supported by the 6th Framework Program of the European Union.

3

References

Aluwihare, L.I., Repeta, D.J., Chen, R.F. 1997. A major biopolymeric component to dissolved organic carbon in surface seawater. Nature 387, 166-169.

Aluwihare, L.I., Repeta, D.J., Chen, R.F. 2002. Chemical composition and cycling of dissolved organic matter in the Mid-Atlantic Bight. Deep-Sea Research II 49, 4421-4437.

Aluwihare, L.I., Meador, T.B. 2008. Chemical composition of marine dissolved organic nitrogen. In: Nitrogen in the Marine Environment, 2nd edition, D.G. Capone, D.A. Bronk, M.R. Mulholland, E.J. Carpenter (eds.), Elsevier, Netherlands pp. 95-133.

Amon, R. M. W; Fitznar, H-P; Benner, R. 2001. Linkages among the bioreactivity, chemical composition, and diagenetic state of marine dissolved organic matter. Limnology and Oceanography 46(2), 287-297.

Amon, R.M.W., Benner, R. 2003. Combined neutral sugar as indicators of the diagenetic state of dissolved organic matter in the Arctic Ocean. Deep-Sea Research I 50, 151-169.

Anderson, L.A., Sarmiento, J.L. 1994. Redfield ratios of remineralization determined by nutrient data-analysis. Global Biogeochemical Cycles 8(1), 65-80.

Arístegui, J., Duarte, C.M., Agustí, S., Doval, M., Álvarez-Salgado, X.A., Hansell, D.A. 2002. Dissolved organic carbon support of respiration in the dark ocean. Science 298, 1967.

Azam, F., Fenchel, T., Field, J.G., Gray, J.S., Meyer-Reil, L.A. and Thingstad, F. 1983. The ecological role of water-column microbes in the sea. Marine Ecology Progress Series 10, 257-263.

Benner, R., Pakulski, J.D., McCarthy, M., Hedges, J.I., Hatcher, P.G. 1992. Bulk chemical characteristics of dissolved organic matter in the ocean. Science 255, 1561-1564.

Benner, R., Biddanda, B., Black, B., McCarthy, M. 1997. Abundance, size distribution, and stable carbon and nitrogen isotopic compositions of marine organic matter isolated by tangential-flow ultrafiltration. Marine Chemistry 57, 243-263.

Béthoux, J.P., Morin, P., Ruiz-Pino, D. 2002. Temporal trends in nutrient ratios: chemical evidence of Mediterranean ecosystem changes driven by human activity. Deep-Sea Research II 49, 2007–2016.

Brix, H., Gruber, N., Karl, D. M., Bates, N. R. 2006. On the relationships between primary, net community, and export production in subtropical gyres. Deep-Sea Research II (53), 698-717.

1 Carlson, C.A. 2002. Production and removal processes. In: Biogeochemistry of Marine
2   Dissolved Organic Matter, D.A. Hansell and C.A. Carlson (eds.), Academic Press, San
3   Diego, pp. 91-139.
4 Carlson, C.A., Ducklow, H.W., Michaels, A.F. 1994. Annual flux of dissolved organic carbon
5   from the euphotic zone in the Northwestern Sargasso Sea. Nature 371, 405-408.
6   1845–1858.
7 Carlson, C.A., Ducklow, H.W. 1995. Dissolved organic carbon in the upper ocean of the central
8   Equatorial Pacific, 1992: Daily and fine-scale vertical variations. Deep-Sea Research II
9   42, 639-656.
10 Carlson, C. A., Hansell, D. A., Nelson, N. B., Siegel, D. A., Smethie, W. M. Jr., Khatiwala, S.,
11   Meyers, M. M., Wallner, E. 2010. Dissolved organic carbon export and subsequent
12   remineralization in the mesopelagic and bathypelagic realms of the North Atlantic basin.
13   Deep Sea Research II, this volume.
14 Carpenter, J. H. 1965(a). The accuracy of the Winkler method for the dissolved oxygen analysis.
15   Limnology and Oceanography, 10, 135-140.
16 Carpenter, J. H. 1965(b). The Chesapeake Bay Institute technique for dissolved oxygen method.
17   Limnology and Oceanography, 10, 141-143.
18 Cherrier, J., Bauer, J.E., Druffel, E.R.M. 1996. Utilization and turnover of labile dissolved
19   organic matter by bacterial heterotrophs in eastern North Pacific surface waters. Marine
20   Ecology Progress Series 139, 267-279.
21   Copin-Montegut, G., Avril, B., 1993. Vertical distribution and temporal variation of
22   dissolved organic carbon in the North-Western Mediterranean Sea. Deep-Sea Research
23   40, 1963-1972.
24 Copin-Montégut, G.C., Avril, B. 1993. Vertical distribution and temporal variation of dissolved
25   organic carbon in then north-western Mediterranean Sea. Deep-Sea Research 40(10),
26   1963-1972.
27 Dauwe, B., Middelburg, J.J., Herman, P.M.J., Heip, C.H.R. 1999. Linking diagenetic alteration of
28   amino acids and bulk organic matter reactivity. Limnology and Oceanography 44(7),
29   1809-1814.
30 De Corte, D., Yokokawa, T., Varela, M.M., Agogué, H., Herndl, G.J. 2009. Spatial
31   distribution of *Bacteria* and *Archaea* and *amo*A gene copy numbers throughout the water
32   column of the Eastern Mediterranean Sea. The ISME Journal 3, 147–158.
33 Doval, M.D., Hansell, D.A. 2000. Organic carbon and apparent oxygen utilization in the western
34   South Pacific and the central Indian Oceans. Marine Chemistry 68, 249-264.

1   Druffel, E.R.M., Bauer, J.E., Williams, P.M., Griffin, S., Wolgast, D. 1996. Seasonal variability
2   of particulate organic radiocarbon in the northeast Pacific Ocean. Journal of Geophysical
3   Research 101 (C9), 20543–20552.
4   Fernandes, V., Ramaiah, N., Paul, J.T., Sardessai, S., Babu R.J., Gaums, M. 2008. Strong
5   variability in bacterioplankton abundance and production in central and western Bay of
6   Bengal. Marine Biology 153, 975-985.
7   Fitznar, H.-P., Lobbes, J.M., Kattner G. 1999. Determination of enantiomeric amino acids with
8   high-performance liquid chromatography and pre-column derivatisation with o-
9   phthaldialdehyde and N-isobutyrylcysteine in seawater and fossil samples (mollusks).
10   Journal of Chromatography 832, (1-2), 123-132.
11 Fukuda, R., Ogawa, H., Nagata, T., Koike, I. 1998. Direct determination of carbon and nitrogen
12   contents of natural bacterial assemblages in marine environments. Applied and
13   Environmental Microbiology 64(9), 3352-3358.
14 Gertman, I., Pinardi, N., Popov, Y., Hecht, A. 2006. Aegean Sea water masses during the early
15   stages of eastern Mediterranean climactic transient. Journal of Physical Oceanograpy 36,
16   1841-1859.
17 Goldberg, S.J., Carlson, C.A., Hansell, D. A., Nelson, N. B., Siegel, D. A. 2009. Temporal
18   dynamics of dissolved combined neutral sugars and the quality of dissolved organic
19   matter in the Northwestern Sargasso Sea. Deep-Sea Research I 56, 672-685.
20 Guo, L., Santschi, P.H., Cifuentes, L.A., Trumbore, S.E., Southon, J. 1996. Cycling of high-
21   molecular-weight dissolved organic matter in the middle Atlantic bight as revealed by
22   carbon isotopic (13C and 14C) signatures. Limnology and Oceanography 41(6), 1242-
23   1252.
24 Hansell, D.A. 2002. DOC in the global ocean carbon cycle. In: Biogeochemistry of Marine
25   Dissolved Organic Matter, D.A. Hansell and C.A. Carlson (eds.), Academic Press, San
26   Diego, pp. 685-715.
27 Hansell, D.A., Carlson, C.A. 2001. Biogeochemistry of total organic carbon and nitrogen in the
28   Sargasso Sea: control by convective overturn. Deep Sea Research II. 48, 1649-1667.
29 Hansell, D.A., Carlson, C.A. 1998a. Deep ocean gradients in dissolved organic carbon
30   concentrations. Nature 395, 263-266.
31 Hansell, D.A., Carlson, C.A. (1998b). Net community production of dissolved organic carbon.
32   Global Biogeochemical Cycles 12, 443-453.

1   Hansell, D.A. 1993. Results and observations from the measurement of DOC and DON in

2   seawater using a high-temperature catalytic oxidation technique. Marine Chemistry 41,

3   195– 202.

4   Hedges, J.I. 1992. Global biogeochemical cycles: progress and problems. Marine Chemistry 39,

5   67-93.

6   Hoehler, T.M. 2004. Biological energy requirements as quantitative boundary conditions for life

7   in the subsurface. Geobiology 2, 205-215.

8   Hubberten, U., Lara, R.J., Kattner, G. 1994. Amino acid composition of seawater and dissolved

9   humic substances in the Greenland Sea. Marine Chemistry 45, 121–128.

10   Ignatiades, L. 1998. The productive and optical status of the oligotrophic waters of the Southern

11   Aegean Sea (Cretan Sea), Eastern Mediterranean. Journal of Plankton Research 20 (5),

12   985 –995.

13   Kaartokallio, H., Kuosa, H., Thomas, D.N., Granskog, M.A., Kivi, K. 2007. Biomass,

14   composition and activity of organism assemblages along a salinity gradient in sea ice

15   subjected to river discharge in the Baltic Sea. Polar Biology 30, 183-197.

16   Kaiser, K., Benner R. 2005. Hydrolysis-induced racemization of amino acids. Limnology and

17   Oceanography Methods. 3, 318-325.

18   Kaiser, K., Benner R. 2008. Major bacterial contribution to the ocean reservoir of detrital organic

19   carbon and nitrogen. Limnology and Oceanography 53(1), 99-112.

20   Kaiser, K., Benner R. 2009. Biochemical composition and size distribution of organic matter at

21   the Pacific and Atlantic time-series stations. Marine Chemistry 113, 63-77.

22   Karageorgis, A.P., Gardner W.D., Gergopoulos, D., Mishonov, A.V., Krasakopoulou, E.,

23   Anagnostou, C. 2008. Particle dynamics in the Eastern Mediterranean Sea: a synthesis

24   based on light transmission, PMC, and POC archives (1991-2001). Deep-Sea Research I

25   55, 177-202.

26   Karner, M., Herndl, G.J. 1992. Extracellular enzymatic activity and secondary production in

27   free-living and marine-snow-associated bacteria. Marine Biology 113, 341-347.

28   Keil, R.G., Kirchman, D.L. 1994. Abiotic transformation of labile protein to refractory protein in

29   sea water. Marine Chemistry 45, 187-196.

30   Kirchman, D., 2001. Measuring bacterial biomass production and growth rates from leucine

31   incorporation in natural aquatic environments. In Methods in Microbiology (Vol 30):

32   Marine Microbiology, J.H. Paul (ed.). Academic Press.

33   Klein, B., Roether, W., Kress, N., Manca, B.B., d'Alcala, M.R., Souvermezoglou, E., Theocharis,

34   A., Civitarese, G., Luchetta, A. 2003. Accelerated oxygen consumption in eastern

Mediterranean deep waters following recent changes in thermohaline circulation. J. Geophysical Research – Oceans 108. doi:10.1029/2002JC001454.

Krasakopoulou, E., Souvermezoglou, E., Pavlidou, A., Kontoyiannis, H. 1999. Oxygen and Nutrient Fluxes through the Straits of the Cretan Arc (March 1994 - January 1995). Progress in Oceanography, 44, 601-624.

Krom, M.D., Groom, S., Zohary, T. 2003. The Eastern Mediterranean. In: Black, K.D., Shimmield, G.B. (Eds.), The Biogeochemistry of Marine Systems. Blackwell Publishing, Oxford, pp. 91–122.

Krom, M.D., Brenner, S., Kress, N., Neori, A., Gordon, L.I. 1992. Nutrient dynamics and new production in a warm-core eddy from the E Mediterranean. Deep-Sea Research 39, 467–480.

Lascaratos, A. 1993. Estimation of deep and intermediate water mass formation rates in the Mediterranean Sea. Deep-Sea Research II 40, 1327–1332.

Lefèvre, D., Denis, M., Lambert, C. E., Miquel, J.-C. 1996. Is DOC the main source of organic matter remineralization in the ocean water column? Journal of Marine Systems 7, 281-291.

Martín-Cuadrado, A.-B., López-García, P., Alba, J.-C., Moreira, D., Monticelli, L., Strittmatter, A., Gottschalk, G., Rodríguez-Valera, F. 2007. Metagenomics of the deep Mediterranean, a warm bathypelagic habitat. . PLoS One 2, e914.

McCarthy, M., Hedges, J., Benner, R. 1996. Major biochemical composition of dissolved high molecular weight organic matter in seawater. Marine Chemistry 55, 281-297.

McCarthy, M., Hedges, J., Benner, R. 1998. Major bacterial contribution to marine dissolved organic nitrogen. Science 281, 231-234.

Meador, T.B., Aluwihare, L. I., Mahaffey, C. 2007. Isotopic heterogeneity and cycling of organic nitrogen in the oligotrophic ocean. Limnology Oceanography 52(3), 934-947.

Meador, T.B. 2008. A spatial deconvolution of molecular signals in oceanic dissolved organic matter. UC San Diego: Scripps Institution of Oceanography. Retrieved from: http://escholarship.org/uc/item/55d4w9xc

Murphy, J., Riley, J. P. 1962. A modified solution method for determination of phosphate in natural waters. Analytica Chimica Acta 27, 31-36.

Myers, P.G., Haines, K. 2000. Seasonal and interannual variability in a model of the Mediterranean under derived flux forcing. Journal of Physical Oceanography 30(5), 1069-1082.

1   Myklestad, S.M., Skanøy, E., Hestmann S. 1997. A sensitive and rapid method for analysis of

2   dissolved mono- and polysaccharides in seawater. Marine Chemistry 56, 279-286.

3   Nagata, T., Fukuda, H., Fukuda, R., Koike, I. 2000. Bacterioplankton distribution and production

4   in deep Pacific waters: Large-scale geographic variations and possible coupling with

5   sinking particle fluxes. Limnology and Oceanography 45, 426-435.

6   Nagata, T., Tamburini, C., Aristegui, J., Baltar, F., Bochdansky, A., Fonda-Unami, S., Fukuda,

7   H., Gogou, A., Hansell, D.A., Hansman, R.L., Herndl, G., Panagiotopoulos, C.,

8   Reintharler, T., Sohrin, R., Verdugo, P., Yamada, N., Yamashita, Y., Yokokawa, T.,

9   Bartlett, D.H. 2010. Emerging concepts on microbial processes in the bathypelagic ocean

10   – ecology, biogeochemistry and genomics. Deep Sea Research II, this volume.

11   Panagiotopoulos, C., Sempéré, R. 2005. Analytical methods for the determination of sugars in

12   marine samples: a historical perspective and future directions. Limnology and

13   Oceanography: Methods 3, 419-454.

14   Pérez, M. T., Pausz, C., Herndl, G.J. 2003. Major shift in bacterioplankton utilization of

15   enantiomeric amino acids between surface waters and the ocean's interior. Limnology

16   and Oceanography 48, 755–763.

17   Psarra, S., Tselepides, A., Ignatiades, L., 2000. Primary productivity in the oligotrophic Cretan

18   Sea (NE Mediterranean): seasonal and interannual variability. Progress in Oceanography

19   46, 187–204.

20   Repeta, D.J., Aluwihare, L.I. 2006. Radiocarbon analysis of neutral sugars in high-molecular-

21   weight dissolved organic carbon: implications for organic carbon cycling. Limnology

22   and Oceanography 51(2), 1045-1053.

23   Roether, W., Klein, B., Manca, B.B, Theocharis, A., Kioroglou, S. 2007. Transient Eastern

24   Mediterranean deep waters in response to the massive dense-water output of the Aegean

25   Sea in the 1990s. Progress in Oceanography, 74, 540-571.

26   Roether, W., Well, R. 2001. Oxygen consumption in the Eastern Mediterranean. Deep-Sea

27   Research I 48, 1535–1551.

28   Santinelli, C., Manca, B.B., Gasparini, G.P., Nannicini, L., Serriti, A. 2006. Vertical distribution

29   of dissolved organic carbon (DOC) in the Mediterranean Sea. Climate Research 31, 205-

30   216.

31   Santinelli , C., Nannicini, L., Seritti, A. 2010. DOC dynamics in meso and bathypelagic layers of

32   the Mediterranean Sea. Deep Sea Research II, this volume.

Sempéré, R., Charrière, B., Van Wambeke, F., Cauwet, G. 2000. Carbon inputs of the Rhône River to the Mediterranean Sea: biogeochemical implications. Global Biogeochemical Cycles 14(2), 669-681.

Sempéré, R., Panagiotopoulos, C., Lafont, R., Marroni, B., Van Wambeke, F. 2002. Total organic carbon dynamics in the Aegean Sea. Journal of Marine Systems 33-34, 355-364.

Seritti, A., Manca, B.B., Santinelli, C., Murru, E., Boldrin, A., Nannicini, L. 2003. Relationships between dissolved organic carbon (DOC) and water mass structures in the Ionian Sea (winter 1999). Journal of Geophysical Research 108. doi:10.1029/2002JC001345.

Skoog, A, Benner, R. 1997. Aldoses in various size fractions of marine organic matter: implications for carbon cycling. Limnology and Oceanography 42 (8): 1803-1813.

Smith, D., Simon, M., Alldredge, A.L., Azam, F. 1992. Intense hydrolytic enzyme activity on marine aggregates and implications for rapid particle dissolution. Nature 359, 139-142.

Spyres, G., Nimmo, M., Worsfold, P.J., Achterberg, E.P., Miller, A.E.G. 2000. Determination of dissolved organic carbon in seawater using high temperature catalytic oxidation techniques. Trends in Analytical Chemistry 19 (8), 498–506.

Stavrakakis, S., Krasakopoulou, E., Kabouri, G., 2006. Particulate organic carbon fluxes and balance estimation in S. Aegean (SE Mediterranean Sea). Proceedings of 8th Panhellenic Symposium of Oceanography and Fisheries, Thessaloniki, 4-8 June 2006, p. 159.

Strickland, J. D. H., Parsons, T. R. 1972. A practical handbook of sea water analysis. Fisheries Research Board of Canada 167, 310p.

Teira, E., v. Aken, H., Veth, C., Herndl, G.J. 2006. Archaeal uptake of enantiomeric amino acids in the meso- and bathypelagic waters of the North Atlantic. Limnology and Oceanography 51, 60-69.

Theocharis, A., Balopoulos, E., Kioroglou S., Kontoyiannis, H., Iona, A. 1999. A synthesis of the circulation and hydrography of the South Aegean Sea and the Straits of the Cretan Arc (March 1994–January 1995). Progress in Oceanography 44, 469-509.

Toggweiler, J.R. 1989. Is the downward dissolved organic matter (DOM) flux important in carbon transport? In 'Productivity in the Ocean: Present and Past' (W.H. Berger, V.S. Smetacek and G. Wafer, Eds.), pp. 65-83. Wiley, New York.

Tzipperman, E., Speer, K. G. 1994. A study of water mass transformation in the Mediterranean Sea: analysis of climatological data and a simple 3-box model. Dynamics of Atmospheres and Oceans 21, 53-82.

1 UNESCO, 1986. Progress on Oceanographic Tables and Standards 1983–1986. Work and
2   recommendations of the UNESCO/SCOR/ICES/IAPSO Joint Panel. UNESCO Technical
3   Papers in Marine Science, 50.

4 Varela, M.M., van Aken, H.M., Sintes, E., Herndl, G.H. 2008. Latitudinal trends of
5   Crenarchaeota and Bacteria in the meso- and bathypelagic water masses of the Eastern
6   North Atlantic. Environmental Microbiology 10(1), 110-124.

7 Wetzel, R. G. 1992. Gradient-dominated ecosystems: sources and regulatory functions of
8   dissolved organic matter in freshwater ecosystems. Hydrobiologia 229, 181-198.

9 Williams, P.M., Druffel, E.R.M. 1988. Dissolved organic matter in the ocean: comments on a
10   controversy. Oceanography 1, 14-17.

11 Yamashita, Y, Tanoue, E. 2003. Distribution and alteration of amino acids in bulk DOM along
12   a transect from bay to oceanic waters. Marine Chemistry, 82 (3-4):145-160.

13 Zervakis, V., Drakopoulos, P.G., Georgopoulos, D. 2000. The role of the North Aegean in
14   triggering the recent Eastern Mediterranean climatic changes. Journal of Geophysical
15   Research 105 (C11), 103-126.

16 Zervakis, V., Georgopoulos, D. 2002. Hydrology and Circulation in the North Aegean (eastern
17   Mediterranean) throughout 1997-1998. Mediterranean Marine Science, 3/1, 5-19.

18 Zervakis, V., Krasakopoulou, E., Georgopoulos D., Souvermezoglou, E. 2003. Vertical diffusion
19   and oxygen consumption during stagnation periods in the deep North Aegean. Deep-Sea
20   Research I 50, 53-71.

21 Zervakis, V., Georgopoulos, D., Karageorgis A. F., Theocharis, A. 2004. On the response of the
22   Aegean Sea to climatic variability: a review. International Journal of Climatology 24,

Figure Captions

Figure 1. UDOM sampling stations (circles) collected during POSEIDON, SESAME, and KM3NET cruises in May 2007 and April 2008.

Figure 2. Temperature-salinity diagrams for stations sampled in the N. Aegean (filled circles), S. Aegean (diamonds), S.W. Aegean (grey circles), and Ionian seas (filled triangles). Enlarged symbols represent stations and depths where water was sampled for ultrafiltration.

Figure 3. AOU versus DOC for all stations of the POSEIDON cruise (open diamonds), and for stations where UDOM was collected (filled diamonds). The dashed line represents the regression for all stations where AOU > 0 $\mu mol\ L^{-1}$.

Figure 4. DOC concentration versus (A & B) picoplankton abundance and (C &D) heterotrophic picoplankton activity observed during the POSEIDON cruise in the N. Aegean (NA, diamonds), Southwest Aegean (SA-W, squares), Ionian (triangles), and S. Aegean Seas (SA, circles). Filled symbols represent stations where UDOM samples were collected, and the dashed lines represent linear regressions that are statistically significant ($p < 0.05$) and include the entire datasets, except in (D), where the regression represents values below 300 m depth.

Figure 5. Characteristic UDOM ^{1}H-NMR spectra at various depths of the North Aegean and Ionian Seas. Sample names are provided for each spectrum; the HDO peak at 4.7 ppm was removed from all spectra.

Figure 6. AOU versus %AA-UDOC (filled symbols) and DCAA concentration (open symbols). The dashed line represents linear regression of the %AA-UDOC data.

Figure 7. Relationship between %AA-UDOC vs. picoplankton abundance (A) and picoplankton activity (B). Note picoplankton abundance and activity are plotted on a logarithmic scale. Dotted lines represent exponential regressions that were statistically significant ($p < 0.002$).

Figure 8. Biplots of PC1 (x-axis) and PC2 loadings (y-axis) of (A) amino acid and (B) monosaccharide distributions in UDOM. Amino acids that plot in clusters identified in (A) are defined in the text.

1

2

3   Figure 9. Average %bacteria-derived DOM as calculated using the formula:

4    $([D\text{-}AA]/[TOC])_{sample}/([D\text{-}AA])/([TOC])_{culture}$, after Kaiser and Benner (2008). Error bars

5   represent one standard deviation.

6

7

8

9

10

11

12

13

14

Table 1. Bulk hydrographic and chemical measurements of seawater collected from ultrafiltration during the Poseidon, Sesame, and KM3Net research cruises. *nd* = no data; σ_θ = sigma-theta density; AOU = apparent oxygen utilization; DOC = dissolved organic carbon.

Cruise	Sample	Date	Lat. (°N)	Lon. (°E)	Depth (m)	Salinity	Temp. (°C)	σ_θ (kg m^{-3})	AOU (μmol L^{-1})	DOC (μmol L^{-1})	Vol. (L) ultrafiltered	% DOC retained, ultrafiltered	% DOC retained, diafiltered*
POSEIDON	N. Aegean	8-May-07	40.109	24.531	2	36.245	17.669	26.309	-8.624	120	185	24	10±1
					200	38.976	14.073	29.255	21.109	62	240	29	28
					1000	39.041	13.353	29.485	59.296	53	150	39	9±1
	S.W. Aegean	11-May-07	36.200	23.308	2	38.759	17.729	28.224	-5.393	84	180	47	33
					500	38.939	14.420	29.161	26.256	54	220	54	40±6
					1200	38.980	14.351	29.232	46.675	52	305	44	39±3
	Ionian	26-May-07	36.265	21.502	2	38.535	21.146	27.149	-4.628	77	300	43	18±2
					250	38.801	15.255	28.858	19.323	65	170	61	37
					750	38.819	14.031	29.161	61.703	50	170	64	17
					4350	38.743	14.190	29.201	48.953	48	170	76	51±3
	S. Aegean	28-May-07	35.787	24.912	2	*nd*	*nd*	*nd*	-8.43	78	210	*nd*	25
					750	38.939	14.389	29.176	35.161	54	210	*nd*	20
					1400	39.040	14.255	29.304	37.823	48	210	*nd*	22
SESAME	N. Aegean NS1	6-Apr-08	40.127	25.305	2	33.802	12.725	25.52	-4.993	120	400	*nd*	15±2
	N. Aegean NS6	9-Apr-08	40.474	24.598	2	35.117	13.413	26.4	-1.284	95	100	*nd*	27±2
KM3Net	Ionian K-C2	17-Apr-08	36.676	21.660	2	38.557	16.049	*nd*	*nd*	82	200	*nd*	19
	Ionian K-4.5	19-Apr-08	36.548	21.459	2	38.575	16.286	*nd*	*nd*	91	150	*nd*	13

* ± error is based on the DOC concentration of ultrafiltered and diafiltered DOC retentates and is shown only for samples with error ≥ 1%.

Table 2. Inorganic and organic nutrients, and picoplankton abundance and activity at the different sampling sites and depths.

Station	Depth (m)	DIN (μmol L^{-1})	DIP (μmol L^{-1})	DON (μmol L^{-1})	Picoplankton ($\times10^5$ cells mL^{-1})	Picoplankton Activity (pmol leu L^{-1} h^{-1})
N. Aegean	2	0.7	0.05	9.7	5.5	110.32
	200	1.9	0.08	6.6	1.6	4.91
	1000	4.6	0.15	4.9	0.6	2.09
S.W. Aegean	2	0.2	0.03	9.7	3.1	48.90
	500	1.2	0.06	5.3	1.2	4.05
	1200	3.9	0.16	5.1	0.6	1.52
Ionian	2	0.1	0.03	5.9	*nd*	27.13
	250	0.8	0.04	10.1	1.2	1.93
	750	3.1	0.15	6.0	0.4	0.10
	4350	4.0	0.15	7.1	0.3	1.16
S. Aegean	2	0.4	0.03	5.3	*nd*	69.33
	750	3.0	0.11	5.2	1.0	8.35
	1400	3.3	0.14	4.5	0.6	2.68

Table 3. Monosaccharide mol % distributions, and % contribution of ^{1}H-NMR regions to spectra of UDOM, sorted by AOU values of waters where seawater was collected. Bold values indicate a significant correlation (r) between AOU and monosaccharide mole % or ^{1}H-NMR component data as defined by the Pearson correlation coefficient. *nd* = no data.

Station	Depth (m)	AOU (µmol L^{-1})	DCNS (µmol C L^{-1})	%NS-UDOC	rham	fuc	arab	xyl	mann	glu	gal	aliphatic	alpha subs	hetero subs
							Monosaccharides mole %						^{1}H-NMR group	
DB2-Athos	2	-8.624	*nd*	*nd*	*nd*	*nd*	*nd*	*nd*	*nd*	*nd*	*nd*	32	28	41
W. Cretan	2	-5.393	*nd*	*nd*	9.4	11.6	5.8	8.7	15.5	20.2	28.8	*nd*	*nd*	*nd*
Ionian	2	-4.628	*nd*	*nd*	8.7	11.1	6.7	9.4	15.9	19.2	29.0	*nd*	*nd*	*nd*
DB8-Cretan	2	-8.843	*nd*	*nd*	12.3	11.9	6.4	5.7	17.8	17.7	28.2	*nd*	*nd*	*nd*
Sesame NS1	2	-4.99	9.1	1.6	9.3	12.4	5.6	8.3	14.9	21.3	28.1	25	26	49
Sesame NS6	2	-1.28	14.3	3.7	9.1	11.7	5.6	7.2	17.7	15.9	32.7	27	29	44
KM3NET C2	2	*nd*	24.3	3.8	10.2	12.2	6.4	6.9	16.6	19.7	28.0	27	30	44
Ionian	250	19.323	10.4	2.5	9.4	11.1	6.4	5.3	17.2	21.7	28.8	33	32	35
DB2-Athos	200	21.109	2.6	0.5	10.2	10.8	5.9	5.9	20.1	20.4	26.7	33	33	34
W. Cretan	500	26.256	2.9	0.6	15.0	14.6	6.1	6.0	15.3	20.3	22.8	34	34	33
DB8-Cretan	750	35.161	4.6	0.5	12.7	12.6	6.7	6.7	16.1	20.1	25.0	33	34	33
DB8-Cretan	1350	37.823	4.3	0.4	12.3	9.2	6.9	5.6	19.2	19.8	27.0	34	35	31
W. Cretan	1200	46.675	2.3	0.5	10.8	11.3	5.7	5.1	20.7	21.7	24.6	35	35	31
Ionian	4350	48.953	7.7	1.9	12.9	14.2	5.9	9.9	16.4	22.1	18.7	33	33	34
DB2-Athos	1000	59.296	*nd*	*nd*	9.5	11.5	5.9	6.3	17.4	24.2	25.2	28	30	42
Ionian	750	61.703	*nd*	*nd*	11.1	10.8	9.0	8.2	16.9	20.7	23.2	34	35	31
r (AOU)	-	-	-0.63	-0.56	0.49	0.01	0.50	-0.12	0.32	**0.54**	**-0.76**	**0.73**	**0.92**	**-0.85**
p	-	-	0.069	0.092	0.075	0.973	0.069	0.683	0.265	**0.046**	**0.002**	**0.003**	**< 0.001**	**< 0.001**

43

Table 4. Amino acid abundance and mol % distributions in UDOM, sorted by AOU values of waters where seawater was collected. Bold values indicate a significant correlation (*r*) between AOU and amino acid mole % data as defined by the Pearson correlation coefficient.

Station	Depth (m)	AOU (μmol O_2 L^{-1})	DCAA (nmol C L^{-1})	%AA-UDOC	asx	D-asx	glx	D-glx	ser	D-ser	thr/his	gly	arg	ala	D-ala	tyr	D-tyr	val	phe	leu
N. Aegean	2	-8.624	461	1.6	12.7	2.6	9.0	2.0	5.5	1.5	8.2	33.0	2.5	8.8	3.1	2.6	0.4	3.6	0.8	3.8
SW Aegean	10	-5.393	581	1.4	14.0	3.9	8.6	2.7	3.9	2.1	5.6	32.2	3.6	8.0	4.4	2.7	0.4	3.2	1.3	3.4
N. Aegean	200	21.109	216	1.2	12.7	4.6	8.2	2.6	3.6	2.1	5.3	36.4	2.9	8.0	4.4	2.2	0.5	3.1	0.3	3.2
SW Aegan	500	26.256	334	1.1	10.5	5.1	8.8	2.7	4.1	2.9	5.7	36.4	1.8	7.7	4.9	2.4	0.6	2.4	1.3	2.5
SW Aegean	1200	46.675	202	0.9	12.1	6.2	10.4	3.0	2.2	1.7	3.4	36.6	3.5	7.2	5.1	2.1	0.3	2.8	0.7	2.6
Ionian	4350	48.953	356	1.0	13.2	5.1	9.7	2.9	2.3	1.3	3.7	34.7	3.9	8.1	4.4	1.8	0.2	3.6	1.4	3.7
N. Aegean	1000	59.296	188	0.9	14.5	3.2	9.6	1.6	3.0	1.0	5.4	33.6	3.5	9.0	2.3	2.1	0.2	4.4	1.7	5.0
Ionian	750	61.703	270	0.8	12.3	5.8	9.1	3.4	2.2	1.6	3.3	37.1	3.9	8.0	4.4	1.8	0.3	2.8	1.0	2.9
r (AOU)			-0.73	**-0.98**	-0.31	**0.89**	0.55	**0.84**	**-0.90**	-0.24	**-0.89**	**0.80**	0.47	-0.55	0.57	**-0.95**	-0.48	-0.33	0.12	-0.49
p			0.063	**< 0.001**	-	**0.007**	-	**0.02**	**0.003**	-	**0.017**	**0.031**	-	-	-	**0.001**	-	-	-	-

Table 5. Correlations of site-specific physical, chemical, and biological parameters with PC1 and PC2 scores derived from PCA of amino acid or monosaccharide mol %. Parameters are groupd according to those that exhibit trends that generally decrease with depth (I), increase with depth (II), or unrelated to depth (III). Z-socres for individual PC are shown in parentheses. Correlations to amino acid concentrations are also shown. All reported correlations are significant to at least $p < 0.05$.

		DCAA	Variability in AA mole distribution		Variability in monos mole distribution	
			PC1 (48%)	PC2 (31%)	PC1 (36%)	PC2 (25%)
I	Temperature	0.88	0.79	-	-	-
	TOC	-	0.91	-	-	0.75
	UDOC	-	-	-	-	-
	DCAA	*na*	-	-	-	0.96
	DCNS	-	-	-	-	0.66
	%AA-UDOC	-	0.96	-	-	-
	%NS-UDOC	-	-	-	-	-
	[1]H hetero-subs	-	0.98	-	-	0.85
	Cells mL-1	-	0.93	-	-	-
	Pico. activity		0.89	-	-	-
	Eubacteria	0.74	-	-	-	-
II	Salinity	-	-0.80	-	-	-0.57**
	σ_t	-	-0.87	-	-	-0.79**
	AOU	-	-0.90	-	-	-0.67**
	Nitrate + Nitrite	-	-0.83	-	-	-
	Phosphate	-	-0.84	-	-	-
	DIN:DIP	-0.79	-0.79	-	-	-
	Σ-D/L	-	-0.83	-	-	-
	[1]H aliphatic	-	-0.91	-	-	-0.85
	[1]H alpha-subs	-	-0.97	-	-	-0.83
III	%DOC retained*	-0.07	-0.62	0.25	0.44	-0.23

* Correlation was determined to examine if UDOC recovery influenced variability in amino acid or monosaccharide distribution. Non-diafiltered UDOC recoveries are used for comparisons related to amino acid analysis and diafiltered UDOC recoveries are used for comparisons of monosaccharide analysis. For all r reported, p > 0.1

** These correlations were significant ($p < 0.05$) but the relationships were driven by surface samples with low salinity and AOU.
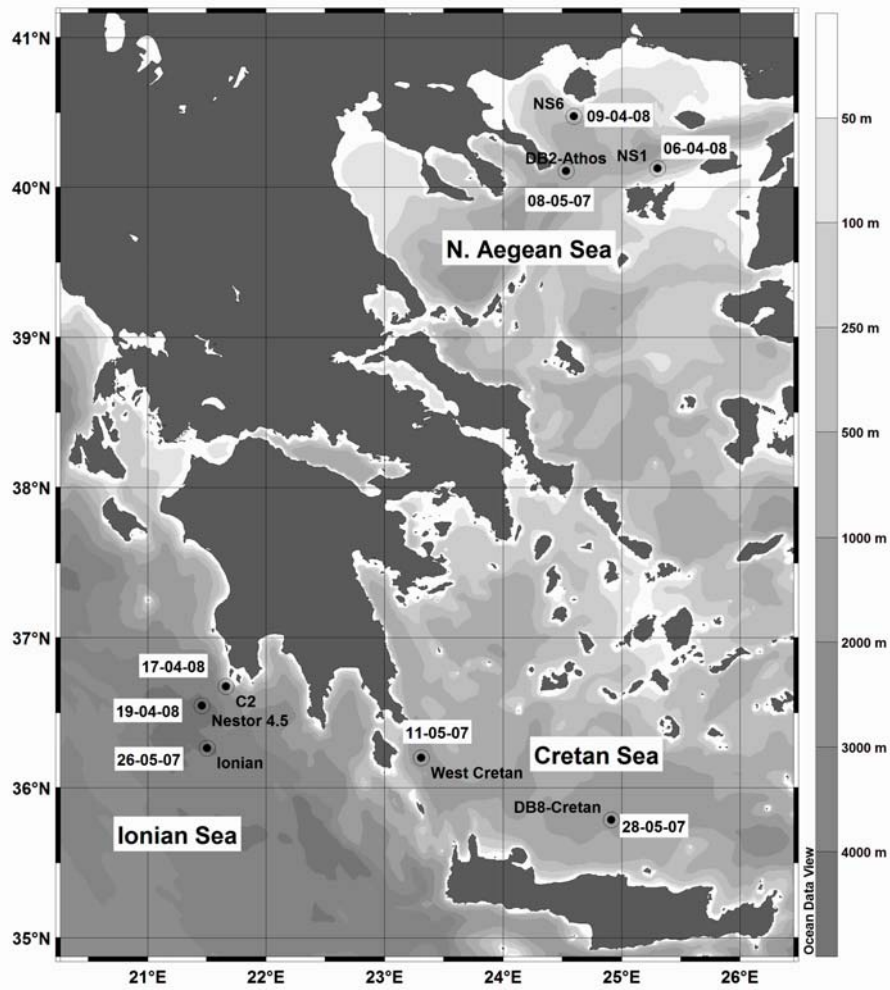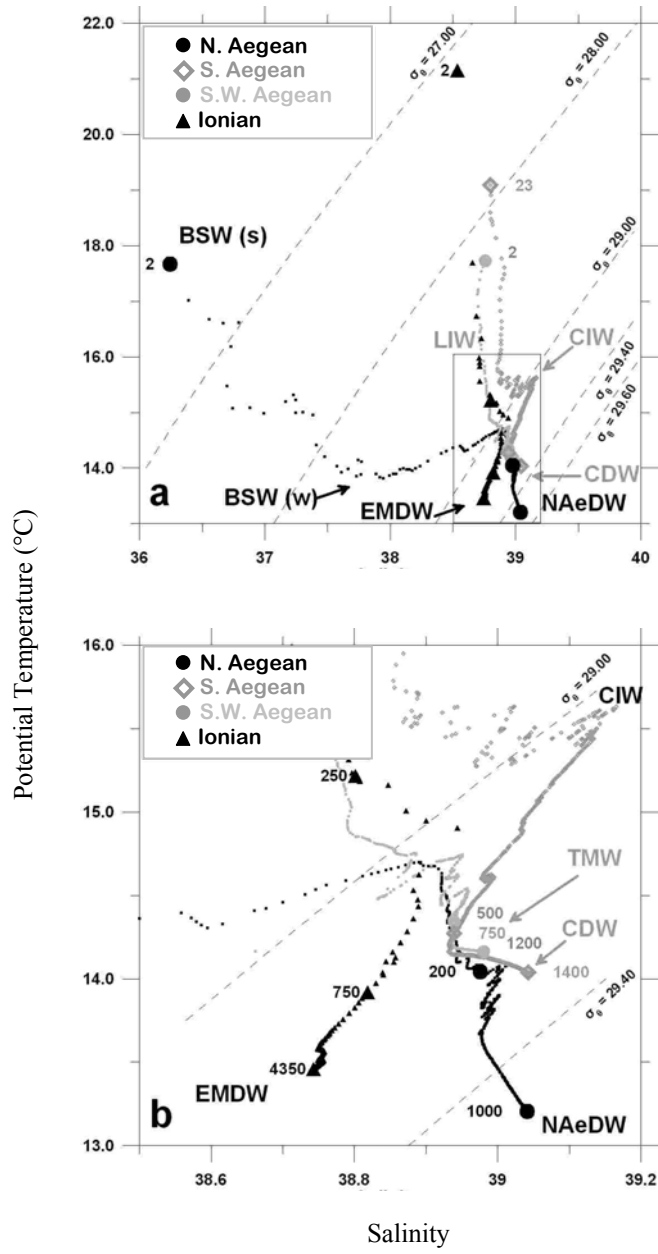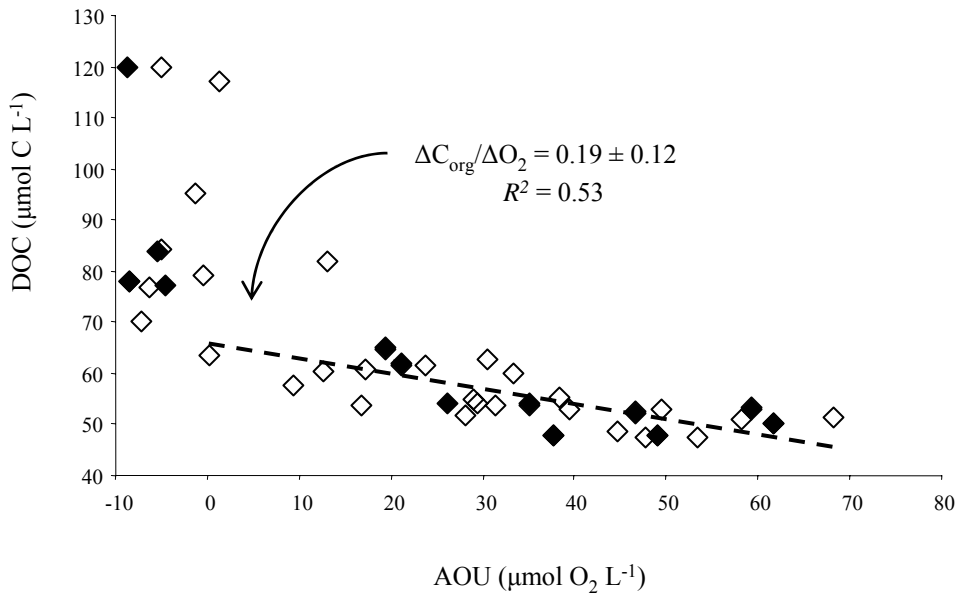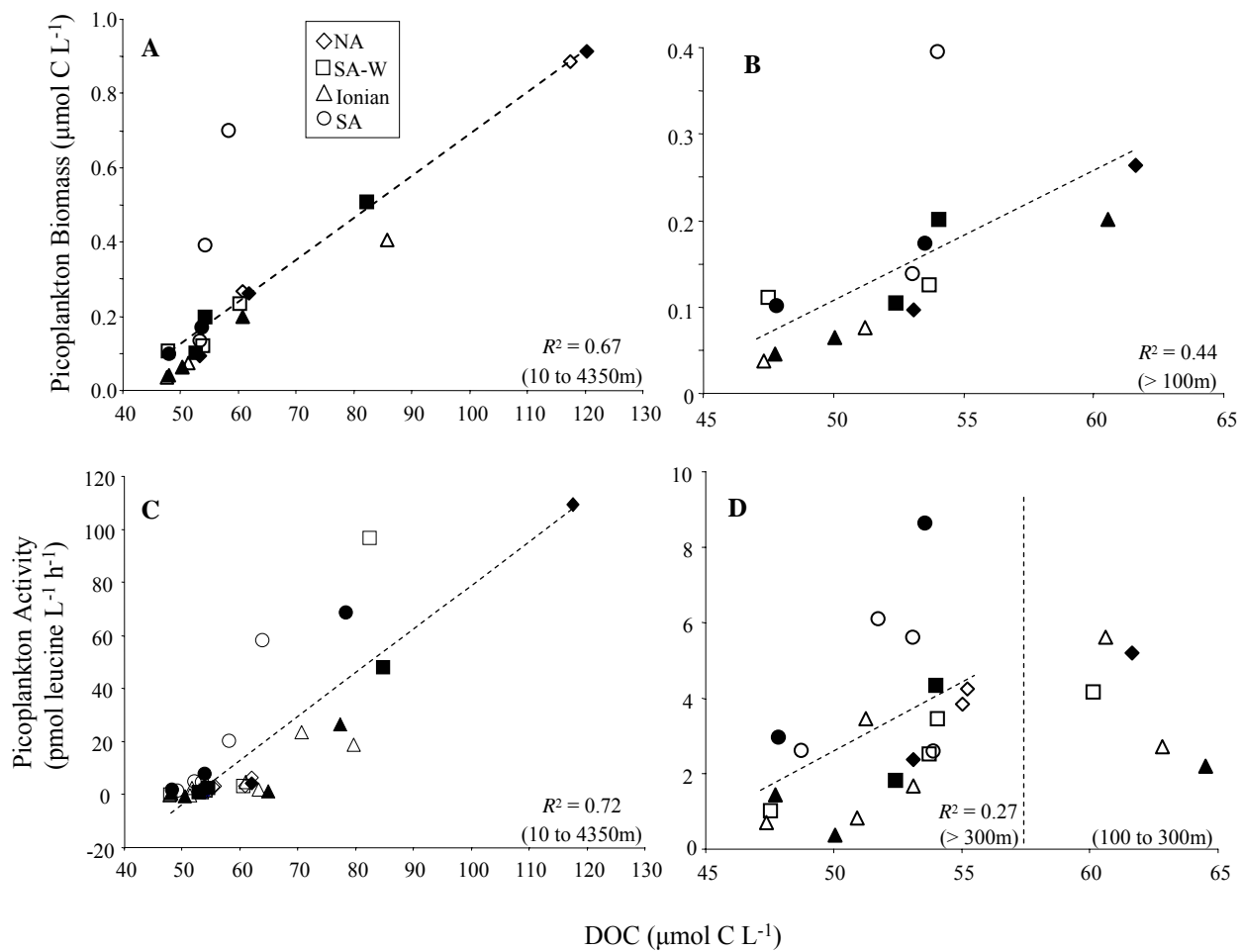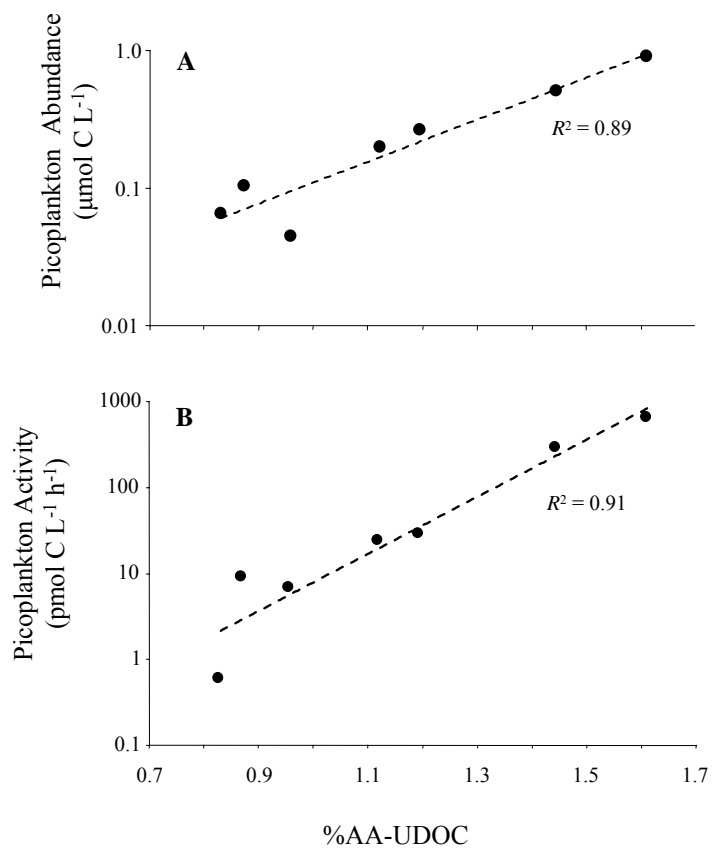
Figure 1.

Figure 2.

Figure 3.

48

Figure 4.

**N. Aegean
2m**

**N. Aegean
200m**

**N. Aegean
1000m**

Ionian
2m

Ionian
250m

Ionian
750m

Ionian
4350m

9 8 7 6 5 4 3 2 1

9 8 7 6 5 4 3 2 1 ppm

Figure 5.

$R^2 = 0.96$

%AA-UDOC

DCAA (nmol L^{-1})

AOU (μmol O$_2$ L^{-1})

Figure 6.

51

Figure 7.

Figure 8

% Bacteria-derived DOM

Depth (m)

Figure 9.